ADA039135

THE UNIVERSITY OF NEW MEXICO
COLLEGE OF ENGINEERING

BUREAU OF ENGINEERING RESEARCH

REPORT DOCUMENTATION PAGE	READ INSTRUCTIONS BEFORE COMPLETING FORM

1. REPORT NUMBER AFOSR - TR - 77 - 0625	2. GOVT ACCESSION NO.	3. RECIPIENT'S CATALOG NUMBER

4. TITLE (and Subtitle) LASER DAMAGE IN SEMICONDUCTORS	5. TYPE OF REPORT & PERIOD COVERED Final rept.
	6. PERFORMING ORG. REPORT NUMBER

7. AUTHOR(s) S K Gulati W W Grannemann	8. CONTRACT OR GRANT NUMBER(s) F44620-75-C-0077 new

9. PERFORMING ORGANIZATION NAME AND ADDRESS Electrical Engineering & Computer Science University of New Mexico Albuquerque NM 87131	10. PROGRAM ELEMENT, PROJECT, TASK AREA & WORK UNIT NUMBERS 9767-04 61102F

11. CONTROLLING OFFICE NAME AND ADDRESS AFOSR/NP Bolling AFB, Bldg.410 Wash DC 20332	12. REPORT DATE Mar 1977
	13. NUMBER OF PAGES 119

14. MONITORING AGENCY NAME & ADDRESS(if different from Controlling Office)	15. SECURITY CLASS. (of this report) Unclassified
	15a. DECLASSIFICATION/DOWNGRADING SCHEDULE

16. DISTRIBUTION STATEMENT (of this Report)

Approved for public release;
distribution unlimited.

17. DISTRIBUTION STATEMENT (of the abstract entered in Block 20, if different from Report)

18. SUPPLEMENTARY NOTES

19. KEY WORDS (Continue on reverse side if necessary and identify by block number)

20. ABSTRACT (Continue on reverse side if necessary and identify by block number)

Experimental damage thresholds for Si, Ge, GaAs, GaAs(x)P(1-x) and GaP have been determined at 10.6 x10 to the -6 and 1.06 x10 to the -6 laser wavelengths. For CW CO(2) laser damage, all the thresholds are of the order of a few kW/cm(2) for an irradiation time of about 0.10 second. At 1.06 x10 to the -6 wavelength and for nanosecond pulses, the damage thresholds are of the order of 10(9) W/cm(2). The damage thresholds can be explained by assuming that the anomalous absorption takes place through the parametric instability of the type formulated by DuBois and Goldman. The plasma concentration required for the onset of this

DD FORM 1473 1 JAN 73   EDITION OF 1 NOV 65 IS OBSOLETE

instability at 10.6 x10 to the -6 is easily achieved by photon induced excitation of the valence electrons to the conduction band through a continuous distribution of Shockley surface states. At 1.06 x 10 to the -6, the required plasma concentration in case of Germanium and Silicon is produced by band to band transitions and by Zener tunneling in case of GaAs, $GaAs_{(x)}P_{(1-x)}$ and GaP. In practice the damage occurs both at the surface of the semiconductor and within the bulk, creating defects that cause carrier removal and mobility degradation. The defects so created are more active at lower temperatures than at room temperature as seen from the experimentally measured Hall mobility versus temperature curves before and after laser damage. Carrier removal and mobility degradation curves appear qualitatively to be similar to those observed for electron, neutron and r-ray damage. These changes in electrical properties can be explained by assuming the creation of localized traps in the band gap and appying the model of James and Lark-Horovitz.

LASER DAMAGE IN SEMICONDUCTORS

by

S. K. Gulati
and
W. W. Grannemann

Technical Report (Final) No. EE-245(77)AFOSR-379-1

March 1977

ACKNOWLEDGEMENTS

ii

ABSTRACT

Experimental damage thresholds for Si, Ge, GaAs, $GaAs_xP_{1-x}$ and GaP have been determined at 10.6 μm and 1.06 μm laser wavelengths. For CW CO_2 laser damage, all the thresholds are of the order of a few kW/cm^2 for an irradiation time of about 0.10 second. At 1.06 μm wavelength and for nanosecond pulses, the damage thresholds are of the order of 10^9 W/cm^2. The damage thresholds can be explained by assuming that the anomalous absorption takes place through the parametric instability of the type formulated by DuBois and Goldman. The plasma concentration required for the onset of this instability at 10.6 μm is easily achieved by photon induced excitation of the valence electrons to the conduction band through a continuous distribution of Shockley surface states. At 1.06 μm, the required plasma concentration in case of Germanium and Silicon is produced by band to band transitions and by Zener tunneling in case of GaAs, $GaAs_xP_{1-x}$ and GaP.

In practice, the damage occurs both at the surface of the semiconductor and within the bulk, creating defects that cause carrier removal and mobility degradation. The defects so created are more active at lower temperatures than at room temperature as seen from the experimentally measured Hall mobility versus temperature curves before and after laser damage. Carrier removal and mobility degradation curves appear qualitatively to be similar to those observed for electron, neutron and γ-ray damage. These changes in electrical properties can be explained by assuming the creation of localized traps in the band gap and applying the model of James and Lark-Horovitz.

iii

TABLE OF CONTENTS

iv

TABLE OF CONTENTS (Concluded)

LIST OF FIGURES

LIST OF FIGURES (Continued)

LIST OF TABLES

LIST OF SYMBOLS

a	Lattice constant
a	A constant defined in Chapter 2
a'	A constant defined in Chapter 2
A	A constant defined in Chapter 2
A	A constant defined in Chapter 4
A'	A constant defined in Chapter 2
b	A constant defined in Chapter 4
B	A constant defined in Chapter 2
B	A constant defined in Chapter 4
c	Velocity of light
$C_{\ell\ell}$	Elastic constant for longitudinal extension in [110] direction
d	Distance
d	Width
d	Thickness
D	Distance
D_o	A characteristic distance defined in Chapter 2
e	Electronic charge
eV	Electron volt
E	Electric field
E_L	Longitudinal electric field
E	Energy
E_g	Band gap
$E_c(k)$	Energy of the conduction band with crystal momentum k

$E_v(k)$	Energy of the valence band with crystal momentum k
E_p	Phonon energy
$E_{p\ell}$	Longitudinal phonon energy
E_{pt}	Transverse phonon energy
E'	Energy as defined in Chapter 2
E'_m	A characteristic energy defined in Chapter 2
E_s	Energy of a trap as measured from the conduction band
E'	Self consistent electric field of a plasma
f	A function defined in Chapter 3
f	Focal length
f_{if}	Oscillator strength
$F(x,y)$	A function defined in Chapter 2
G	Reciprocal lattice vector
h	Planck's constant
$\hbar$	$h/2\pi$
H	Magnetic field
I	Intensity
I_o	Original intensity
I	Current
j	Current density
k	Crystal momentum
k	Wave vector
k_B	Boltzmann constant
k_D	Inverse Debye length
k_z	Crystal momentum in z direction
k_{min}	Minimum crystal momentum at the conduction band minima

k_{max}	Maximum crystal momentum at the valence band maxima
K	Kinetic energy
K_t	Mass action constant defined in Chapter 4
ℓ	Linear dimension of a crystal
L	Lorentz correction factor
m	Mass
m_e	Electron mass
m_i	Ion mass
m_e^*	Electron effective mass
m_j	Mass of species j
m_h^*	Hole effective mass
m_h	Hole mass
n	Electron concentration
n_i	Intrinsic carrier concentration
n_{eff}	Effective number of collisions
N	Number density of charged scattering centers
N_A	Acceptor density
N_D	Donor density
N_o	Number density of molecules
N_I	Number density of ionized impurities
N_n	Number density of neutral impurities
N_t	Total number of transitions
N_t	Total number of traps
$N(E)dE$	Density of states with energy between E and E + dE
$p_{||}$	Polarizability of a molecule parallel to the electric field

$p_\perp$	Polarizability of a molecule perpendicular to the electric field
p	Hole density
P	Polarization vector
P_k	Probability of an interband transition
P_L	Longitudinal polarization
$P^{n\ell}$	Nonlinear polarization
P_o	Power
P_{th}	Threshold power
r	A constant defined in Chapter 3
r	Position vector
$\dot{r}$	Velocity
R	Reflection coefficient
R	Hall constant
$R_{AB,\ CD}$	$\dfrac{\left(V_A - V_B\right)}{I_{CD}}$
s	Radius
s_e	Electron thermal velocity
T	Transmission coefficient
T	Tunnelling probability
T	Temperature in degree Kelvin
T_e	Electron temperature
T_i	Ion temperature
v	Velocity
v_E	Velocity of the electron under an electric field E
v_i	Velocity of the species i

V	Potential energy
V_o	Original volume
w	Tunnelling probability
W	Energy
x	A variable defined in Chapter 2
y	A variable defined in Chapter 2
Z	Nuclear charge
Z	Power absorbed
α	Absorption coefficient
α_A	Absorption coefficient for transitions involving absorption of a phonon
α_d	Absorption coefficient due to direct transitions
α_E	Absorption coefficient involving emission of a phonon
α_I	Absorption coefficient due to indirect transitions
β	A constant defined in Chapter 2
β_n	Real part of the frequency
β	Bulk compressibility
γ	A constant defined in Chapters 4 and 5
γ_n	Imaginary part of frequency
δE_c	Shift in the conduction band energy
δV	Differential volume
ε_o	Permittivity of free space
ε	Dielectric constant
ε_L	Longitudinal dielectric constant
ε_L^{NL}	Nonlinear longitudinal dielectric constant

θ	Scattering angle
θ	Beam divergence
θ	Angle between the electric field and direction of propagation of an electromagnetic wave
θ_o	A characteristic angle defined in Chapter 2
θ_d	A characteristic angle defined in Chapter 2
κ	Imaginary part of refractive index
λ	Wavelength
λ'	A constant defined in Chapter 3
Λ	A constant defined in Chapter 2
μ	Mobility
μ_c	Conductivity mobility
μ_H	Hall mobility
μ_e	Electron mobility
μ_h	Hole mobility
μ_I	Mobility due to ionized impurities
μ_t	Total electron mobility
μ_ℓ	Mobility due to lattice scattering
ω_g	Frequency corresponding to band gap
ω	Frequency ($2\pi\nu$)
ω_o	Characteristic frequency
ω_n	Frequency
$d\Omega$	Solid angle element
ν	Frequency
ν_c	Collision frequency
ρ	Resistivity

σ	Conductivity
σ_o	dc conductivity
$\sigma(\theta)$	Scattering cross section
τ	Lifetime
τ_e	Electron lifetime
τ_h	Hole lifetime
χ	Susceptibility tensor
χ_1, χ_2	Factors defined in Chapter 2
η'	Deformation potential constant
η	Refractive index
η_o	Real part of refractive index
ψ	Wave function

CHAPTER 1

INTRODUCTION

The study of the numerous ways in which radiation and matter can interact has been a subject of intensive research for several years. The interaction can be linear or nonlinear depending upon the properties of matter and radiation. The end result of the interaction is mechanical or electrical damage to the matter.

There have been numerous studies of radiation induced damage in semiconductors due to electrons [1, 2, 3], neutrons [4, 5, 6], deutrons [7, 8, 9], α-particles [10, 11] and γ-rays [2, 12]. The study of radiation induced damage in electrical properties of semiconductors is of great importance and is, therefore, a subject of continuous research in solid state electronics.

The present study of laser induced damage in semiconductors was undertaken for several important reasons. Unlike the extensive data available on particle and γ-ray damage, a literature survey shows that only meager and incomplete data exist on laser damage of semiconductors. Today more and more semiconductor devices are finding applications in a wide variety of fields such as in laser systems, laser energy conversion [13], air force weapons, satellites (exposed solar cells), IR controlled weapons, optoelectronics and micro-optics. Therefore, a knowledge of the behavior of the electronic properties of semiconductors under the effect of laser radiation is essential.

_____

*Numbers in brackets refer to references at the end of each chapter.

1

Next, the great structural sensitivity of semiconductors to radiation makes them very useful systems in which to investigate the nature of laser damage in solids. The observed laser induced changes in electrical properties such as carrier mobility, lifetime and concentration can be used to diagnose the damage mechanisms that cause catastrophic material failure in optical materials for high power lasers. For obvious reasons, such techniques cannot be applied to metals and insulating dielectrics.

The damage to semiconductor materials can occur through a number of mechanisms. Chapter 2 describes some of the more important mechanisms through which a laser beam can interact with the semiconductor matter. The absorption of energy can take place through linear processes like band to band transitions, free and bound carrier excitation, lattice absorption or it can occur through nonlinear processes, e.g., avalanche mechanism, self-focusing or plasma instabilities. Most of these mechanisms are described in detail in this chapter.

Chapter 3 gives the theory of the Hall effect as applied by Van der Pauw to determine the carrier mobility in semiconductors. The experimental details regarding the fabrication of devices and the experimental setup to determine mobility, carrier concentration and conductivity are given. Since radiation damage can alter the lattice structure and introduce extra-scattering centers, the theory of different types of scattering mechanisms is also included in this chapter.

Experimental results on CW CO_2 laser damage in different

2

semiconductors are given in Chapter 4. It is shown that the experimental damage thresholds can be explained [14] by applying the theory of parametric instability as formulated by DuBois and Goldman [15]. The observed mobility and carrier concentration changes are explained [16] by applying the model of James and Lark-Horovitz [17].

Chapter 5 gives the experimental results on damage thresholds for semiconductors for Nd:YAG laser (wavelength 1.06×10^{-6} m). The theory of parametric instability again explains the damage thresholds quite well. It is shown that the results of modified two beam instability of Kaw and Dawson [18] do not explain the observed damage thresholds. The theory of photon-plasmon instability of Gersten and Tzoar [19] is also applied to calculate the damage thresholds for different semiconductors, and it is seen that the theory does not predict the damage thresholds correctly. These two instabilities have been used incorrectly by Shatas et al. [20] to explain the damage thresholds for GaAs at CO_2 laser wave length.

3

REFERENCES

1. H. Y. Fan and K. Lark-Horovitz, Semiconductors and Phosphors, Edited by M. Schon and H. Welker, Interscience 1958, p. 113.

2. J. W. Cleland, J. H. Crawford and D. K. Holmes, "Effects of Gamma Radiation on Germanium," Phys. Rev. 102, 722 (1956).

3. J. W. Mackay, E. E. Klontz and G. W. Gobeli, "Thermal and Radiation Annealing of Ge," Phys. Rev. Letters 2, 146 (1959).

4. J. W. Cleland, J. H. Crawford and J. C. Pigg," Fast-Neutron Bombardment of n-Type Ge," Phys. Rev. 98, 1742 (1955).

5. J. W. Cleland and J. H. Crawford, Jr., "Radiation Effects in Indium Antimonide," Phys. Rev. 93, 894 (1954).
    Also see J. W. Cleland and J. H. Crawford, Jr., "Neutron Irradiation of Indium Antimonide," Phys. Rev. 95, 1177 (1954).

6. K. Lark-Horovitz in Semiconducting Materials, edited by H. K. Henisch (Academic Press, Inc., New York 1951) p. 47.

7. J. H. Forster, H. Y. Fan and K. Lark-Horovitz, "Conductivity of Deutron Irradiated Germanium and Silicon," Phys. Rev. 86, 643 (A) (1952).

8. J. H. Forster, "Nucleon Irradiation of Semiconductors," Ph.D. Thesis, Purdue University, 1953.

9. J. H. Forster, H. Y. Fan and K. Lark-Horovitz, "Neutron Irradiation of Germanium Near Liquid Nitrogen Temperature," Phys. Rev. 91, 229 (A) (1953).

10. W. H. Brattain and G. L. Pearson, "Changes in Conductivity of Germanium Induced by Alpha-Particle Bombardment," Phys. Rev. 80, 846 (1950).

11. K. Lark-Horovitz, The Present State of Physics, (American Association for the Advancement of Science, Washington, D. C., 1954) p. 57.

12. H. Y. Fan and K. Lark-Horovitz, The Effect of Radiation on Materials, Edited by J. J. Harwood, H. H. Hanzner, J. G. Morse and W. G. Ranch, Reinhold, 1958, p. 159.

13. R. J. Stirn and Y. C. M. Yeh, "Solar and Laser Energy Conversion with Schottky Barrier Solar Cells," 1974 Proc. IEEE 10th Photovoltaic Specialists Conference, California, USA.

14. S. K. Gulati and W. W. Grannemann, Laser Induced Damage in Optical Materials 1976, Editors A. J. Glass and A. H. Guenther, N.B.S. Special Publication 462, Washington, D. C. (1976) p. 357.

4

15. D. F. DuBois and M. V. Goldman, "Parametrically Excited Plasma Fluctuations," Phys. Rev. $\underline{164}$, 1, 207 (1967).

16. S. K. Gulati and W. W. Grannemann, "Laser (CW CO_2) Induced Electrical Damage in Ge and Si," to be published in Journal of Applied Physics, Manuscript No. 2975R.

17. H. M. James and K. Lark-Horovitz, "Localized Electronic States in Bombarded Semiconductors," Z. Physik. Chem. $\underline{198}$, 107 (1951).

18. P. K. Kaw and J. M. Dawson, "Laser Induced Anomalous Heating of a Plasma," The Physics of Fluids $\underline{12}$, 2586 (1969).

19. J. I. Gerstan and N. Tzoar, "Parametric Excitation of Plasma Instabilities in Semiconductors," Phys. Rev. Letters $\underline{27}$, 1650 (1971).

20. R. A. Shatas J. D. Stettler, L. M. Narducci, S. S. Mitra and H. C. Meyer, Laser Induced Damage in Optical Materials, Editors A. J. Glass and A. H. Guenther, N. B. S. Special Publication 414, Washington, D. C. (1974) p. 200.

CHAPTER 2

FUNDAMENTAL DAMAGE MECHANISMS

This chapter describes the possible mechanisms via which electro-magnetic radiation energy can be absorbed by matter, particularly by semiconductors. When the energy absorbed by a semiconductor exceeds a certain level, mechanical or electrical damage can occur. This energy is called the damage threshold of that semiconductor. Here mechanical damage means any sign of burning of the surface or pit formation or any other visible change in the appearance of the semiconductor surface. Electrical damage stands for any changes in carrier mobility, carrier concentration or carrier lifetime.

The following damage mechanisms will be described:

1. Band to band transitions

2. Free carrier, bound carrier and lattice absorption

3. Avalanche mechanism

4. Self focusing

5. Plasma instabilities.

Here it should be pointed out that this list is by no means intended to be complete and exhaustive.

1. BAND TO BAND TRANSITIONS [1]

The probabilities associated with band to band transitions were first calculated by Kane [2] in 1962, and the theoretical predictions were promptly verified by Allen and Gobeli [3]. The absorption through a transition from valence band to conduction

6

band of a semiconductor is called fundamental absorption.

Two types of transitions must be distinguished. Those in which only a photon is involved are called direction transitions, while those in which both a photon and a phonon are involved are called indirect transitions. In indirect transitions, phonons help conserve the momentum. Below, direct transitions in both direct and indirect band gap semiconductors will be considered.

Direct Transitions (Direct Band Gap $k_{max} = k_{min}$)

In any transition crystal momentum must be conserved. Hence in a direct band gap semiconductor only vertical transitions will be allowed (Figure 2-1). The minimum frequency of the photon that
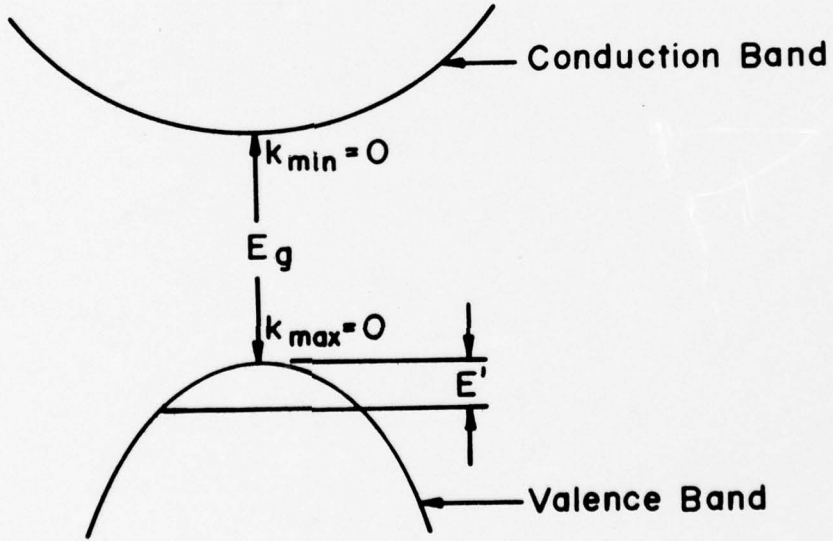
Figure 2-1. A vertical transition in a direct band gap semiconductor

7

can induce such a transition is given by

$$h\nu = E_c(\vec{k}) - E_v(\vec{k}) \tag{2.1}$$

Assuming that the conduction band stays flat near $k = 0$, then $E_c(k)$ in the vicinity of $k = 0$ can be taken as a constant. Differentiating Equation 2.1, we get

$$hd\nu = - dE_v(\vec{k})$$

$$= - d(-E_g - E')$$

or $\quad hd\nu = dE' \tag{2.2}$

where the energy E_g is being measured from the bottom of the conduction band and E' from the top of the valence band.

Now the number of transitions $N_t d\nu$ in the interval $d\nu$ can be written as

$$N_t d\nu = P_k N(E') dE' \tag{2.3}$$

where P_k is the probability associated with the transition and $N(E')dE'$ is the density of states in the energy interval E' and $E' + dE'$. For a parabolic band

$$N(E') = A\sqrt{E'} \tag{2.4}$$

where A is a constant determined by the nature of the semi-conductor.

From Equations 2.3 and 2.4, one can write

$$N_t d\nu = P_k AE'^{\frac{1}{2}} dE' \tag{2.5}$$

From Figure 2-1, we have

$$E' = h\nu - E_g$$

$$\therefore \quad N_t d\nu = AP_k(h\nu - E_g)^{\frac{1}{2}} h \cdot d\nu \tag{2.6}$$

8

From Equation 2.6, one can write the absorption coefficient for a direct transition as

$$\alpha_d = A'P_k(h\nu - E_g)^{\frac{1}{2}}$$

which can also be written as

$$\left. \begin{aligned} \alpha_d &= B(h\nu - E_g)^{\frac{1}{2}} & h\nu &> E_g \\ &= 0 & h\nu &< E_g \end{aligned} \right\} \tag{2.7}$$

The value of B has been found quantum-mechanically by Bardeen, Blatt and Hall [4] and is given by

$$B = \frac{\pi e^2 (2m_r)^{3/2}}{\eta c h^2 m \epsilon_o} f_{if} \tag{2.8}$$

where η is the real part of the refractive index and m_r is the reduced mass of the electron effective mass and hole effective mass given as

$$\frac{1}{m_r} = \frac{1}{m_e^\star} + \frac{1}{m_h^\star}$$

f_{if} is called oscillator strength and is usually of the order of unity.

If $m_e^\star = m_h^\star = m$, then for $\eta = 4$

$$\alpha_d = 6.7 \times 10^4 (h\nu - E_g)^{\frac{1}{2}} f_{if} (cm^{-1}). \tag{2.9}$$

Direct Transitions (Indirect Band Gap $k_{max} \neq k_{min}$)

The band structure of an indirect band gap semiconductor is shown in Figure 2-2.

9
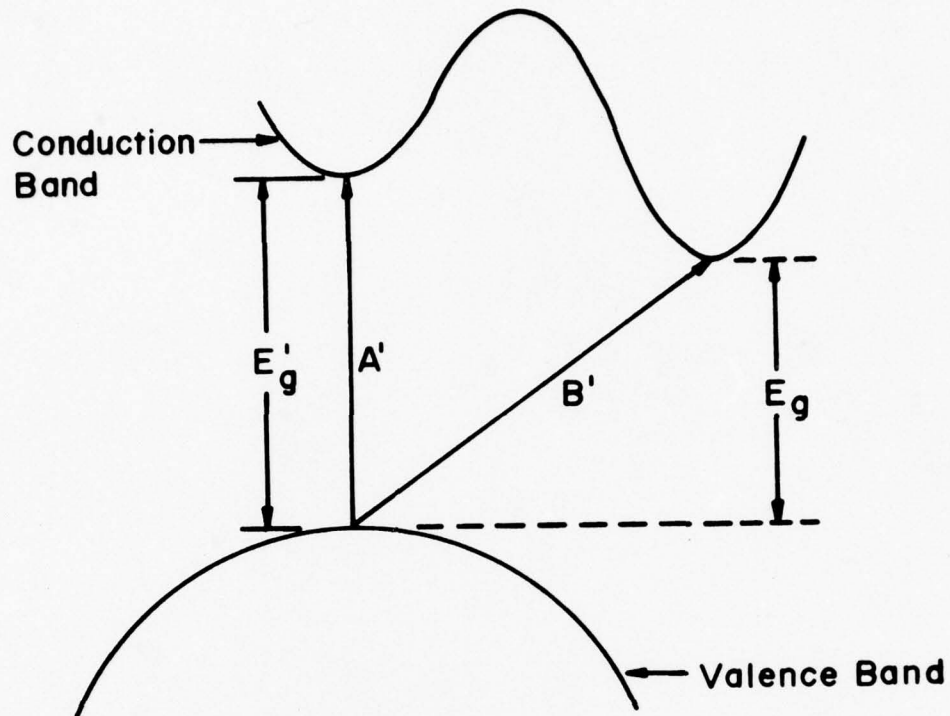
Figure 2-2. A direct (A') and an indirect (B')
transition in an indirect band
gap semiconductor

In this case the maxima of the valence band and minima of
the conduction band lie at different values of k.

The absorption curve for Ge has been obtained by Macfarlane
et al. [5] and is shown in Figure 2-3. The peak in the absorp-
tion curve is due to a vertical transition of the type A' and an
exciton line. The absorption at longer wave lengths is due to
the indirect transitions of the type B' and the momentum is con-
served by emission or absorption of one or more phonons.
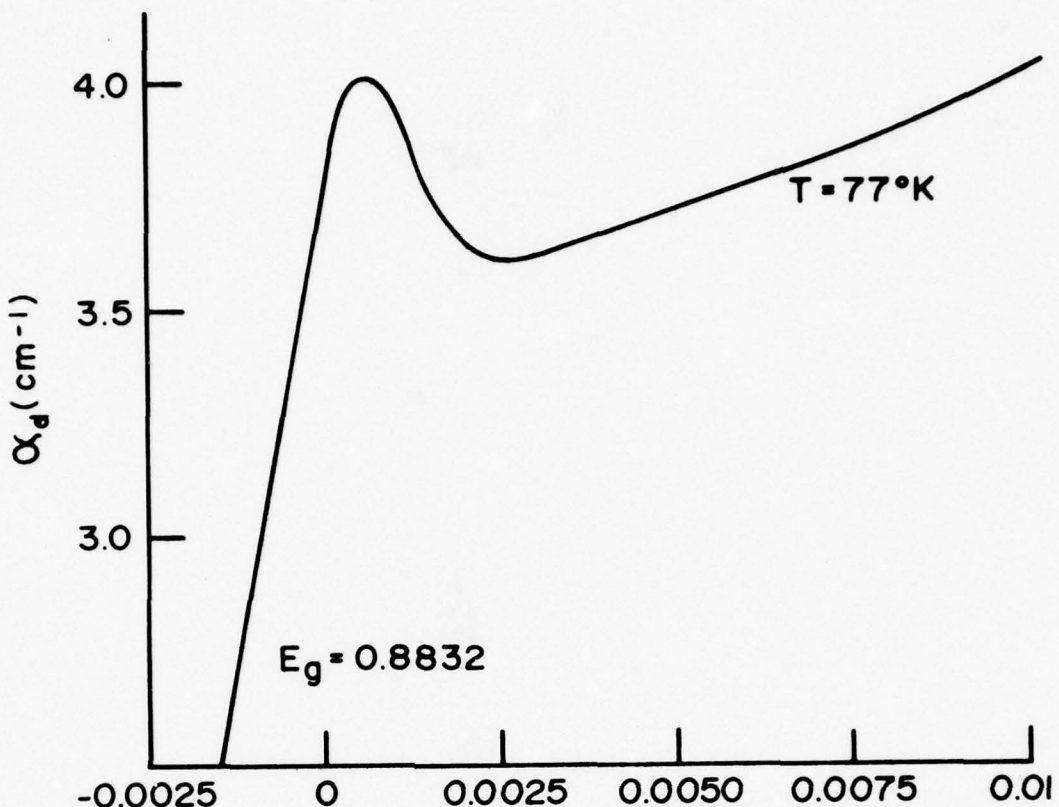
Figure 2-3. Absorption in Ge due to vertical
transitions at k = 0

Indirect Transitions ($k_{min} \neq k_{max}$)

As noted earlier, in indirect transitions one or more phonons
must be involved to conserve the crystal momentum. Therefore, the
minimum photon energy required for such transitions is given by

$$h\nu = E_g - E_p \qquad\qquad (2.10)$$

or $h\nu = E_g + E_p \qquad\qquad (2.11)$

Equation 2.10 implies absorption while Equation 2.11 implies
emission of a phonon in the process.

11

The absorption coefficients for such transitions have been theoretically obtained by Bardeen et al. [5]. Though their formula does not separate the contributions arising from the emission or absorption of phonons, it does take into account the two possible ways in which a transition from a state in the valence band to a state in the conduction band can take place. This is shown in Figure 2-4.
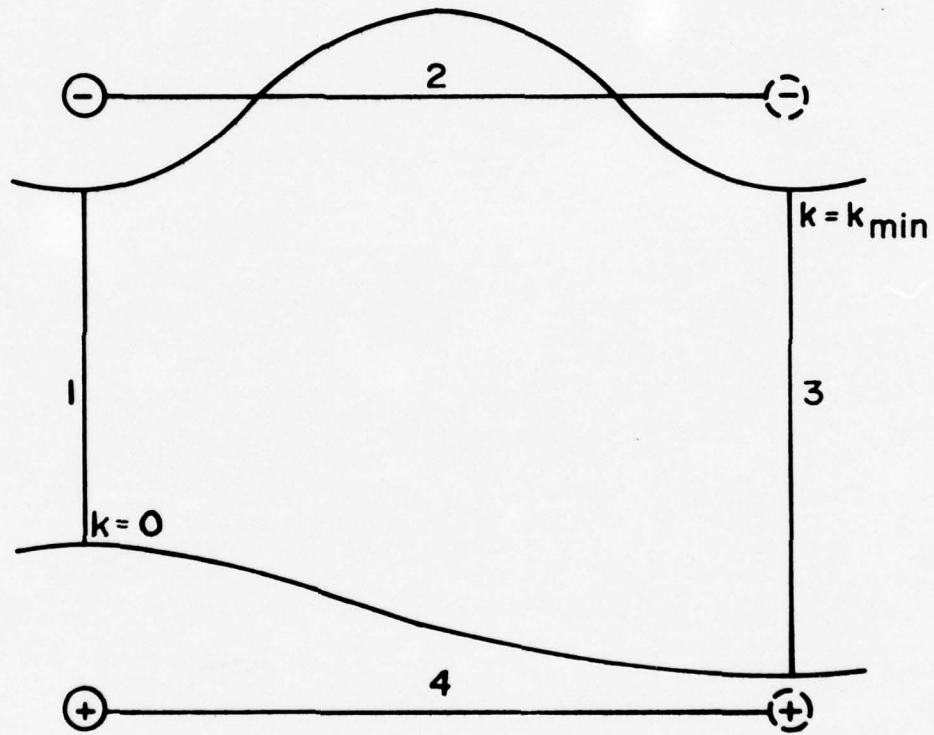
Figure 2-4. Indirect transitions from the valence band to the conduction band

Transition 1 corresponds to an electron excited from the valence band to the conduction band without significant change

in crystal momentum. Since in this state of the conduction band the electron has higher energy, it makes a transition 2 to the state of lower energy in the conduction band with the emission of a phonon of momentum k_{min}. Alternatively an electron may be excited from a state in a valence band to a state in the conduction band through transition 3. The hole left in the valence band then makes a transition to a state near the maxima of the valence band by emission or absorption of a phonon.

To determine the total absorption coefficient one must add the contribution from the transitions involving the absorption of a phonon or emission of a phonon.

$$\alpha_I = \alpha_E + \alpha_A \tag{2.12}$$

where α_I is the total absorption coefficient due to indirect transitions, α_E and α_A are the absorption coefficients due to indirect transitions involving the emission and absorption of a phonon respectively.

From Equations 2.10 and 2.11, we see that

$$\alpha_E = 0 \qquad \text{for } h\nu < E_g + E_p \tag{2.13}$$

$$\alpha_A = 0 \qquad \text{for } h\nu < E_g - E_p \tag{2.14}$$

If $k = 0$ and k_{min} are well separated, then the transition probability between a state near the top of the valence band and a state near the bottom of the conduction band will vary only slightly with k and may be considered as a constant. The total absorption coefficient will then be determined by the density of states from which the transitions are taking place and the relative

13

probability of emission or absorption of a phonon of energy E_p.
The energy E_p will be nearly $\hbar k_{min}$ and can be treated as constant.

The conservation of energy for such transitions requires

$$h\nu = E_g \pm E_p + E + E' \tag{2.15}$$

where E is the energy of the electron above the conduction band
and E' is the energy below the valence band. If E' is fixed,
then

$$h d\nu = dE \tag{2.16}$$

The number of states in the conduction band in this energy
interval is given by

$$\begin{aligned} N_c(E)\,dE &= aE^{\frac{1}{2}}dE \\ &= a(h\nu - E_g \pm E_p - E')^{\frac{1}{2}}dE \end{aligned} \tag{2.17}$$

where a is a constant.

Now the total number of the pairs of states between which
the transitions lying in the interval ν and $\nu + d\nu$ are allowed
can be found by integration over all E' satisfying Equation 2.15.
From Equation 2.15, the maximum value of E' is given by

$$E'_m = h\nu - E_g \pm E_p \ . \tag{2.18}$$

For the density of states of the valence band in the inter-
val dE' we have $a'E'^{\frac{1}{2}}dE'$. Hence the required number of pairs of
states is given by integrating Equation 2.17

$$\begin{aligned} N(\nu)\,d\nu &= aa'h d\nu \int_0^{E'_m} (E'_m - E')^{\frac{1}{2}} E'^{\frac{1}{2}}dE' \\ &= D{E'_m}^2 d\nu \end{aligned} \tag{2.19}$$

where D is a constant.

14

For the absorption of a phonon

$$E_m' = h\nu - E_g + E_p$$

and, therefore,

$$N(\nu)d\nu = D(h\nu - E_g + E_p)^2 d\nu \tag{2.20}$$

Phonons are Bose particles and the probability that a phonon will have an energy E_p is given by

$$N_p(E_p) = \frac{1}{\exp(E_p/k_B T) - 1} \tag{2.21}$$

so that the absorption coefficient α_A is given as

$$\left. \begin{aligned} \alpha_A &= \frac{A'(h\nu - E_g + E_p)^2}{\exp(E_p/k_B T) - 1} && \text{for } h\nu > E_g - E_p \\[2mm] &= 0 && \text{for } h\nu < E_g - E_p \end{aligned} \right\} \tag{2.22}$$

where A' is a constant.

Similarly we can show that

$$\left. \begin{aligned} \alpha_E &= \frac{A'(h\nu - E_g - E_p)^2}{1 - \exp(-E_p/k_B T)} && \text{for } h\nu > E_g + E_p \\[2mm] &= 0 && \text{for } h\nu < E_g + E_p \end{aligned} \right\} \tag{2.23}$$

Hence

$$\left. \begin{aligned} \alpha_I &= A'\frac{(h\nu - E_g - E_p)^2}{1 - \exp(-E_p/k_B T)} + \frac{(h\nu - E_g + E_p)}{\exp(E_p/k_B T) - 1} && h\nu > E_g + E_p \\[2mm] &= A'\frac{(h\nu - E_g + E_p)^2}{\exp(E_p/k_{BT}) - 1} && E_g - E_p < h\nu < E_g + E_p \\[2mm] &= 0 && h\nu \leq E_g - E_p \end{aligned} \right\} \tag{2.24}$$

15

The phonon considered in the above treatment can either be an acoustic or an optical phonon. In each mode it can either be a longitudinal or transverse type. This will split the absorption curve into four parts. Using the analysis given above, the values of longitudinal and transverse acoustic phonon energies for Ge have been found [6] to be as E_{pt} = 0.008 eV, and $E_{p\ell}$ = 0.027 eV. In the case of Ge the absorption due to optical phonons is negligible.

For Si, both acoustic and optical phonons give appreciable contribution to the absorption. The phonon energies have been found to be

Acoustic Phonons E_{pt} = 0.0185 eV, $E_{p\ell}$ = 0.0575 eV

Optical Phonons E_{pt} = 0.120 eV, $E_{p\ell}$ = 0.091 eV

A more exact treatment of absorption due to direct and indirect transitions has been given by Fan [7].

Transitions Involving Surface States

If the surface state density is high and the lifetime of these states is long, then an appreciable absorption can take place through surface states. The quantum yields for such processes have been calculated by Kane [2] and can be very high.

2. FREE CARRIER ABSORPTION [18]

When the incident photon energy is not enough to cause band to band transitions, energy can still be absorbed due to intraband transitions. This is called free carrier absorption. Absorption due to intraband transitions is proportional to the

16

number of free carriers in the band.

In the non-degenerate case, semiclassical treatment can be applied to the problem of free carrier absorption. The equation of motion of a free carrier in an alternating electric field of the incident wave can be written as

$$m^* \dot{\vec{v}}(t) = -e\vec{E}(t) \tag{2.25}$$

where m^* is the effective mass of the free carrier and v its velocity under the action of the applied delectric field $\vec{E}$.

In the presence of randomizing collisions Equation 2.25 will be modified to

$$m^* \left(\dot{\vec{v}}(t) + \frac{\vec{v}(t)}{\tau} \right) = e\vec{E}e^{-i\omega t} \tag{2.26}$$

where τ is the appropriate relaxation time of the carriers in the semiconductor. The charged carrier under the action of the applied harmonic field $\vec{E}e^{-i\omega t}$ will be forced to oscillate with a velocity

$$\vec{v}(t) \sim \vec{v}e^{-i\omega t}$$

Substituting this in Equation 2.26 and solving for v, one gets

$$\vec{v} = \frac{-e\vec{E}}{m^* \left(\frac{1}{\tau} - i\omega\right)} \tag{2.27}$$

The current density can now be written as

$$\vec{j} = ne\vec{v}$$

$$= \frac{ne^2\tau}{m^*(1 - i\omega\tau)} \vec{E} \tag{2.28}$$

where e is the charge on the carrier (electron or hole).

17

From Equation 2.28, one can write for the conductivity as

$$\sigma(\omega) = \frac{ne^2\tau}{m^*}\left(\frac{1}{1 - i\omega\tau}\right)$$

$$= \sigma_o\left(\frac{1}{1 - i\omega\tau}\right) \tag{2.29}$$

where σ_o is the dc conductivity of the carrier species.

Following a similar procedure and assuming $r \sim r_o e^{-i\omega t}$, one can solve Equation 2.26 for r and then write the polarization vector

$$\vec{P} = ne\vec{r}$$

$$= \frac{-ne^2}{m^*(\omega^2 + i\omega/\tau)}\vec{E}$$

Now the dielectric constant $\varepsilon(\omega)$ is given by

$$\varepsilon(\omega) = 1 + \frac{P}{E}$$

$$= 1 + \frac{ne^2}{-m^*(\omega^2 + i\omega/\tau)} \tag{2.30}$$

or

$$\varepsilon(\omega) = 1 - \frac{\sigma_o}{\tau(\omega^2 + i\omega/\tau)} \tag{2.31}$$

Rewriting Equation 2.31,

$$\varepsilon(\omega) = 1 - \left(\frac{\sigma_o \tau}{1 + \omega^2\tau^2}\right) + i\frac{\sigma_o}{\omega(1 + \omega^2\tau^2)} \tag{2.32}$$

The real part of this dielectric constant when equated to zero, gives the resonance frequency of the carrier plasma and can be shown

$$\omega_p = \sqrt{\frac{4\pi ne^2}{m^*}} \tag{2.33}$$

18

The imaginary part gives the damping rate of the electromagnetic wave or the absorption coefficient, which in this case is

$$\alpha = \left(\frac{\sigma_o \tau}{1 + \omega^2 \tau^2} \right) \frac{1}{\eta c \epsilon_o} \tag{2.34}$$

where η is the real part of the refractive index, c the velocity of light and ϵ_o is the permittivity of free space.

Now two cases arise:

(a) $\omega\tau >> 1$, which is true for most IR frequencies

$$\alpha = \left(\frac{\sigma_o}{\omega^2 \tau^2} \right) \frac{1}{\eta c \epsilon_o}$$

Substituting

$$\tau = \frac{m^\star \mu_c}{e}$$

and

$$\sigma_o = ne\mu_c \;,$$

$$\alpha = \frac{ne^3}{\omega^2 m^{\star 2} \mu_c \eta c \epsilon_o} \tag{2.35}$$

This equation shows that the absorption coefficient for free carriers is directly proportional to the carrier concentration and the square of the wavelength.

(b) For very low frequencies $\omega\tau << 1$
and, therefore

$$\alpha = \frac{\sigma_o}{\eta c \epsilon_o}$$

$$= 3.75 \left(\frac{\epsilon_o}{\epsilon} \right)^{\frac{1}{2}} \sigma_o \; cm^{-1} \tag{2.36}$$

where ϵ is the dielectric constant of the semiconductor.

19

Expressions 2.35 and 2.36 have been experimentally verified by
by Gibson [9].

Bound Carrier Excitation

Materials that are characterized by a band gap show a low
frequency tail of the fundamental absorption. This absorption co-
efficient can be expressed as
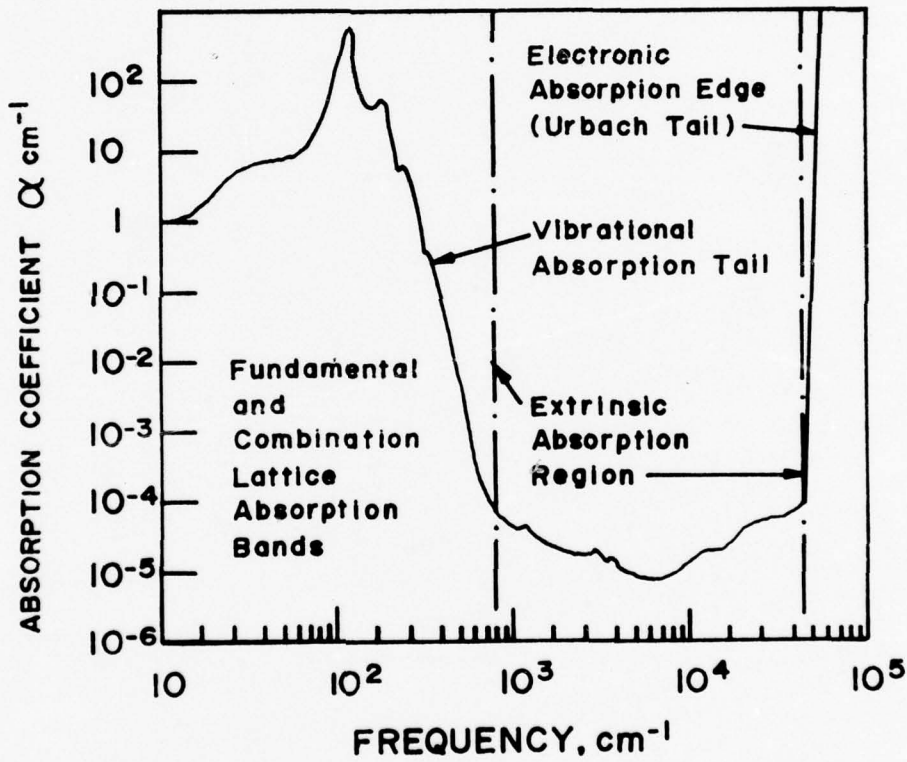
Figure 2-5. Optical absorption versus optical frequency
for a typical material (After Reference [10])

20

$$\alpha(\omega) = A \exp[\beta(\hbar\omega - \Gamma_g)/k_B T] \qquad (2.37)$$

where A and β are constants. This expression is called Urbach's rule [10, 11]. There have been several theoretical attempts to explain this result and none of them is satisfactory. The most recent attempt to explain this effect is by Dow and Redfield [12].

The Urbach tail is usually very steep and can produce significant absorption for those materials whose band gap is not more than 20 $k_B T$ above the frequency which one wants to transmit [13]. This is shown in Figure 2-5.

Lattice Absorption

The vibration spectrum of diatomic lattices has two branches, namely acoustic and optical. The electric field of the incident electromagnetic wave can excite optical vibrations in the lattice, thereby causing strong absorption at the resonance frequency. A number of investigations have shown that the absorption coefficient can be written as [14]

$$\alpha(\omega) = A e^{-\omega/\omega_o} \qquad (2.38)$$

where ω_o is of the order of Restrahl frequency and varies with lattice temperature. The presence of impurities can cause extra absorption by providing different modes of vibration in the crystal. An excellent review of the current work is given in Reference [15].

3. AVALANCHE MECHANISM [16, 17]

The approximate equality between the rms field of the laser

pulse and the dc breakdown field of several alkali halides and other band gap materials has led Bloembergen [17] to believe that the process of laser induced breakdown is electron avalanche similar to the dc avalanche breakdown of reverse biased p-n junctions.

This theory is an extension of Shockley's dc avalanche mechanism. A few "lucky electrons" undergo momentum reversing collisions just in time to be further accelerated by the reversed field of the laser pulse. In other words the collision time of the electron is an odd integral multiple of the half period of the laser pulse.

The equation of motion of an electron in the presence of collisions can be written as

$$m^\star_e \ddot{\vec{r}} + e\vec{E}e^{-i\omega t} + \nu_c m^\star_e \dot{\vec{r}} = 0 \tag{2.39}$$

where $\vec{E}e^{-i\omega t}$ is the laser field, ν_c is the collision frequency of the electron in the crystal lattice and $m^\star_e$ is the effective mass of the electron.

Solving Equation 2.39 for $\dot{r}$ produces

$$\dot{\vec{r}} = -\frac{e}{m^\star_e} \vec{E} \left(\frac{\exp(-i\omega t)}{-i\omega + \nu_c} \right) \tag{2.40}$$

The rate at which an electron moving with the above velocity extracts energy from the electron is given by

$$\dot{W} = \frac{1}{2} \operatorname{Re}(\dot{\vec{r}} \cdot e\vec{E}^\star)$$

$$= \frac{1}{2} \operatorname{Re} \left[-\frac{e^2}{m^\star_e} \frac{E^2}{(-i\omega + \nu)} \right] \tag{2.41}$$

$$= \frac{\nu_c e^2 E^2}{2m^\star_e (\nu_c^2 + \omega^2)}$$

22

Now writing

$$\nu_c = \frac{e}{m_e^* \mu_e} \quad ,$$

therefore,

$$\dot{W} = \frac{\mu e E^2}{(1 + \omega^2 \tau^2)} \tag{2.42}$$

where E can be considered as rms electric field of the laser.

When the energy gained by the electron exceeds the band gap of the material, it will cause further ionization. This process will keep multiplying till the electron concentration is $10^{17} \sim 10^{18}$ cm^{-3}, which gives an exponential contribution to the index of refraction

$$(\eta + i\kappa) = \frac{2\pi e^2 \tau (i - \omega\tau)}{\eta_o m_e^* \omega (1 + \omega^2 \tau^2)} \; n \; \exp\left[\int_o^t \alpha(E)\,dt\right] \tag{2.43}$$

where η_o is the linear index of refraction and $\alpha(E)$ is the electric field dependent ionization rate. n is the original number of electrons per unit volume. The exponential absorption eventually causes damage.

The application of this process to explain laser damage thresholds for semiconductors has recently been questioned by Shatas et al. [18].

4.   SELF-FOCUSING [19, 20, 21, 22, 23]

For most purposes, the refractive index of a substance can be specified as a single number. However, it is well known that the refractive index is dependent on temperature, wavelength and electric field. When a medium is sufficiently absorbing, the

23

refractive index has to be represented as a complex number.

An applied electric field polarizes a medium. The simplest case is when the polarization is proportional to the applied electric field. It can be mathematically stated as

$$\vec{P} = \epsilon_o \chi \vec{E} \qquad (2.44)$$

where χ is known as the susceptibility of the medium. In an anisotropic medium χ may be different in different directions and has to be expressed as a tensor quantity. In Equation 2.44, χ is independent of the electric field. For very high electric fields, local polarization cannot be neglected and, therefore, χ would become a function of the applied electric field. However, the dependence of $\vec{P}$ on $\vec{E}$ must be such that it reduces to Equation 2.53 for low electric fields. Also as $\vec{E}$ reverses, $\vec{P}$ should reverse too. In other words $\vec{P}$ can be a function of only odd powers of $\vec{E}$. Hence one can write,

$$\vec{P}^{n\ell} = \epsilon_o \left(\chi_1 + \chi_2 E^2 + \chi_3 E^4, \ldots \right) \vec{E} \qquad (2.45)$$

Neglecting $\chi_3 E^4$ and higher order terms in the nonlinear polarization,

$$\chi_{eff} = \chi_1 + \chi_2 E^2 \qquad (2.46)$$

Now the refractive index is given by

$$\eta_{eff} = (1 + \chi_{eff})^{\frac{1}{2}}$$

$$= (1 + \chi_1)^{\frac{1}{2}} + \frac{1}{2} \frac{\chi_2}{(1 + \chi_1)^{\frac{1}{2}}} E^2$$

or $\quad \eta_{eff} = \eta_o + \eta_2 E^2 \qquad (2.47)$

24

where η_o is the linear refractive index and

$$\eta_2 = \frac{\chi_2}{2(1 + \chi_1)^{\frac{1}{2}}} = \frac{\chi_2}{2\eta_o}$$

is the nonlinear part of the refractive index and under ordinary circumstances it is very small. For very high electric fields the nonlinear contribution to the refractive index can become significant and cause self-focusing as explained below.

Consider the behavior of light rays on the boundary of a beam having a rectangular distribution as shown in Figure 2-6. Let 2S be the width of the beam.
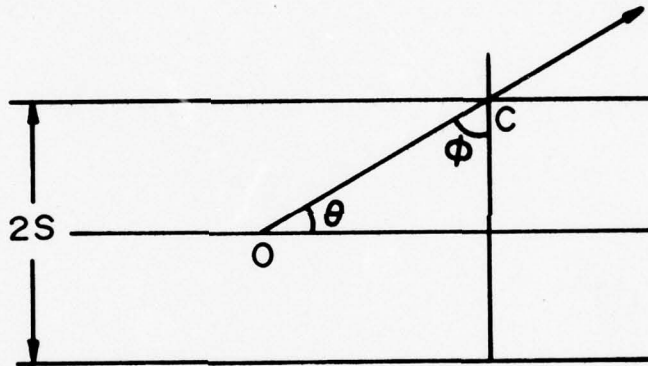
Figure 2-6. A rectangular em wave of width 2s

The refractive index of the medium inside the beam can be written as Equation 2.47

$$\eta = \eta_o + \eta_2 E^2.$$

Outside the beam, the refractive index is simply η_o.

A ray of light starting from 0 will suffer total internal reflection at C, if

25

$$\theta_o = \cos^{-1}\left(\frac{\eta_o}{\eta_o + \eta_2|E|^2}\right) \tag{2.48}$$

θ_o, however, is limited due to diffraction and for a beam of diameter $2s$ it is given as

$$\theta_d = \frac{1.22\lambda}{2\eta_o s} \tag{2.49}$$

Depending on the value of θ_o, the following three cases arise.

(a) $\theta_o < \theta_d$

In this case the beam would spread.

(b) $\theta_o = \theta_d$

In this case the beam would not spread and would get self-trapped.

(c) $\theta_o > \theta_d$

The beam would converge or be self focused.

Case (b) determines the threshold power for self focusing.

i.e. $\theta_o = \theta_d$

or

$$\cos^{-1}\left(\frac{\eta_o}{\eta_o + \eta_2|E|^2}\right) = \frac{1.22\lambda}{2\eta_o s}$$

or

$$\frac{\eta_o}{\eta_o + \eta_2|E|^2} = \cos\left(\frac{1.22\lambda}{2\eta_o s}\right) = 1 + \frac{1}{2}\left(\frac{1.22\lambda}{2\eta_o s}\right)^2$$

or

$$|E|^2 = \frac{\eta_o}{2\eta_2}\left(\frac{1.22\lambda}{2\eta_o s}\right)^2 \tag{2.50}$$

26

Hence the threshold power for self focusing can be written as

$$P_{th} = \frac{c}{8\pi} (\pi s^2) \eta_o |E|^2$$

$$= \frac{c}{64\eta_2} (1.22\lambda)^2 \qquad (2.51)$$

For CS_2, $\eta_2 = 10^{-11}$ ESU

then at

$$\lambda = 0.7 \times 10^{-4} \text{ cm}$$

$$P^{th} \simeq 50 \text{ kW}$$

Such powers are easily obtainable in modern day lasers.

The nonlinear refractive index η_2 can be due to several causes. The three main contributions to η_2 come from

(a) Thermal

(b) Electrostriction

(c) Kerr Effect.

(a) Thermal [24]

Heating of a material causes density changes which according to Clausius Mossoti relation would change the refractive index. Thermal contribution to η_2 is negative and, therefore, causes defocusing action.

(b) Electrostriction [25]

Electrostriction is the mechanical deformation caused by the electric field of the optical beam. This causes an increase in density and, therefore, an increase in the refractive index. The contribution to η_2 in this case is positive and causes self-focusing. This effect is very important in solids.

27

c)   <u>Kerr Effect</u> [26]

The increase in η_2 due to Kerr effect is very important in liquids with anisotropic molecules. The optical field of the laser beam produces an alignment effect on these molecules. It can be shown that

$$\eta_2 = \frac{2\pi(p_{||} - p_\perp)N_o}{35k_B T\eta_o} \cdot L \qquad\qquad (2.52)$$

where

$$L = \frac{(n_o^2 + 2)^4}{81}$$

is the Lorentz local field correction factor. N_o is the number density of the molecules, $p_{||}$ and $p_\perp$ are respectively the principal polarizabilities of the molecule parallel and perpendicular to the electric field of the laser beam.

Once the self focusing action starts, the laser beam will have to travel a certain distance through the medium before it will come to focus. It can be shown that this distance is given by [22]

$$D = D_o \left(1 - \frac{P_{th}}{P_o} \right)^{-\frac{1}{2}} \qquad\qquad (2.53)$$

where

$$D_o = s \sqrt{\frac{\eta_o}{\eta_2 E^2}}$$

and P_o is the power of the optical beam.

Let

$$P_o = 2P_{th}, \text{ then}$$

28

$$D = \sqrt{2} \; D_o \; .$$

Now if

$$E_1 = 10^7 \; V/cm$$
$$n_2 = 10^{-11} \; ESU$$

and if $s = 1$ cm for a CO_2 laser, then

$$D_o \sim 10 \; cm$$

so that

$$D = 14.14 \; cm.$$

The above analysis shows that self focusing would be very unimportant for semiconductor materials, where the thicknesses involved are only a few microns.

It should be noted that a beam can never be focused to a geometric point due to diffraction effects.

5.   PLASMA INSTABILITIES [27, 28]

In high mobility semiconductors electrons and holes can be treated as free particles of an effective mass m*, interacting with each other through coulomb forces. Such a system can be treated like a plasma if the potential energy V due to the coulomb interaction and the kinetic energy K obey

$$\frac{V}{K} \lesssim 1 \tag{2.54}$$

Such a condition is easily satisfied in most semiconductors and, therefore, semiconductors can be assumed to be containers of electron and hole plasmas. A plasma has its characteristic frequency given by

29

$$\omega_p = \sqrt{\frac{4\pi n e^2}{\epsilon m^*}} \tag{2.55}$$

Whenever the frequency of an interacting electromagnetic wave is close to this plasma frequency, several different types of instabilities can be excited due to the resonance effect. A brief description of two of the important instabilities relevant to the present work is given below.

Two Stream Instability [29, 30]

This instability has been treated by Nishikawa [29] and also by Kaw and Dawson [30]. This type of instability can occur in a plasma in which the ions are stationery and the electrons are moving relative to it.

The basic equations of motion of ions and electrons are the continuity equation and the momentum conservation relations as given below.

$$\frac{\partial n_j}{\partial t} + \nabla \cdot (n_j v_j) = 0 \tag{2.56}$$

$$m_j n_j \left(\frac{\partial v_j}{\partial t} + v_j \cdot \nabla v_j \right) = -\nabla p_j + n_j e_j (E \sin\omega t + E')$$
$$- m_j n_j v_j \nu_j \tag{2.57}$$

where ∇p_j gives the pressure gradient, E' the self consistent field of the electrons and the ions and all other terms have their usual meaning.

Finally E' is given by the Poisson's equation

$$\nabla \cdot E' = 4\pi \sum_j e_j n_j \tag{2.58}$$

Assuming that n_j (the ion density) is a slowly varying function

30

of time and neglecting

$$\frac{m_e}{m_i} ,$$

one can solve [30] the above equations to get the following fourth

order dispersion relation for ω

$$1 = \omega_p^2 \left[\frac{m_e}{m_i \omega^2} + \frac{1}{(\omega - kv_o)^2} \right] \tag{2.59}$$

where v_o is the relative velocity of electrons w.r.t. ions and k is

the wave vector of the electromagnetic wave. If all the roots

of Equation 2.59 are real, then each root would indicate a pos-

sible oscillation given by

$$E' \propto e^{i(\vec{k} \cdot \vec{r} - \omega_n t)} \tag{2.60}$$

If some of the roots are complex, then they would occur in

conjugate pairs. Let these roots be written as

$$\omega_n = \beta_n + i\gamma_n \tag{2.61}$$

The time dependence of the E-field will now be given as

$$E' \propto e^{i(\vec{k} \cdot \vec{r} - \omega_n t)} \cdot e^{\gamma_n t} \tag{2.62}$$

Equation 2.62 suggests that the electrostatic wave can grow

exponentially if γ_n is positive. This would give rise to the two

stream instability.

Rewriting Equation 2.59, by putting

$$x = \frac{\omega}{\omega_p}$$

and

$$y = \frac{kv_o}{\omega_p}$$

31

$$1 = \frac{m_e/m_i}{x^2} + \frac{1}{(x-y)^2} F(x,y) \tag{2.63}$$

For any given value of y, one can plot $F(x,y)$ as a function of x. This function would have poles at $x = 0$ and $x = y$ as shown in Figure 2-7.
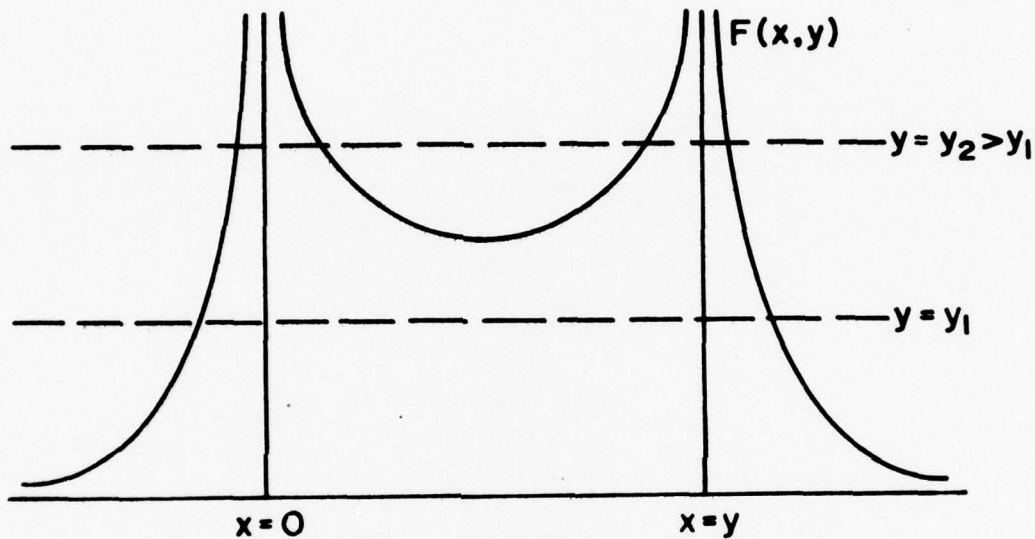
Figure 2-7. Function $F(x,y)$ in the two stream instability

For $y = y_2 > y$, the line $F(x,y) = 1$ cuts the curve at four points corresponding to four real roots. However, for $y = y_1$, only two roots are real and the other two must be complex, giving rise to an unstable wave in the plasma. This would happen for small y, i.e. for small kv_o. With the help of the dispersion relation it can be shown that the maximum growth rate of this instability is given by

32

$$I_m\left(\frac{\omega}{\omega_p}\right) = \left(\frac{m_e}{m_i}\right)^{1/3}$$

(2.64)

Kaw and Dawson [31] further show that the roots of the dispersion relation are complex, i.e. the instability occurs if

$$\frac{eE}{m_e\omega} \geq \sqrt{2}\sqrt{\frac{k_B T_e}{m_e}}\left(1 + \frac{T_i}{T_e}\right)^{\frac{1}{2}}$$
$$\left(1 - \frac{\omega^2}{\omega_R^2}\right)^{\frac{1}{2}} \cdot \left(1 + \frac{\nu_e^2}{\omega_R^2\left(1 - \frac{\omega^2}{\omega_R^2}\right)}\right)^{\frac{1}{2}}$$

(2.65)

where T_i and T_e are the ion and electron temperatures and can be assumed to be equal in case of semiconductors. Hence Equation 2.65 can be written as

$$\therefore \quad \frac{eE}{m_e\omega} \geq 2\sqrt{\frac{k_B T}{m_e}}\left(1 - \frac{\omega^2}{\omega_R^2}\right)^{\frac{1}{2}}\left(1 + \frac{\nu_e^2}{\omega_R^2\left(1 - \frac{\omega^2}{\omega_R^2}\right)}\right)^{\frac{1}{2}}$$

(2.66)

Here $\omega_R = \sqrt{\omega_p^2 + k^2\frac{k_B T_e}{m_e}}$

(2.67)

Now if $\omega \sim \omega_R \sim \omega_p$, Equation 2.66 gives

$$\frac{eE}{m_e\omega} > 2\sqrt{\frac{k_B T}{m_e}}\left(\frac{\nu_e}{\omega_R}\right)$$

(2.68)

Converting Equation 2.68 into power threshold

$$P_{th} = \eta_o \frac{c}{8\pi}\left(\frac{\nu_e}{\omega_R}\right)^2 \cdot 4 \cdot \left(\frac{k_B T}{m_e}\right)\frac{m_e^2\omega^2}{e^2}$$

$$= \frac{c\eta_o}{2\pi}\nu_e^2\frac{m_e}{e^2}\left(\frac{\omega}{\omega_R}\right)^2 \cdot (k_B T)$$

(2.69)

33

An application of this equation to calculate the damage threshold for CO_2 lasers and for Nd:YAG laser gives results that are 2 to 3 orders higher than the observed damage thresholds.

Parametric Instability

This type of instability was originally formulated by DuBois and Goldman [31, 32, 33, 34] and later has been treated by several other authors [35, 36, 37].

This instability arises if one feeds energy to the plasma at a rate faster than it can dissipate it. Parametric instability arises when an intense laser beam of frequency ω_o interacts with the plasma of resonance frequency ω_R. If $\omega_o - \omega_R$ is close to the ion acoustic frequency or ion optical frequency ω_L, the ion waves will absorb energy resonantly. Similarly ω and ω_L can interact to pump the electron plasma.

Therefore, monochromatic pump radiation of the form

$$\frac{1}{2} \vec{E}_o [\exp i(\vec{k}_o \cdot \vec{r} - \omega_o t) + c \cdot c]$$

will modulate the plasma at the beat frequencies $\omega \pm \omega_o$ [31]. The longitudinal polarization in a medium under the action of the laser field will be a function of the fields at $\omega \pm \omega_o$ frequencies. The modulation of the longitudinal polarization can be neglected at all other frequencies. Therefore, inside the medium

$$-E_L(k,\omega) = P_L(k,\omega) = E_L(k,\omega)\chi_L(\vec{k},\omega) + \vec{E}_o \cdot \chi_L^{NL}(\vec{k}_o,\omega_o;\vec{k}-\vec{k}_o,\omega-\omega_o) \cdot$$

$$E_L(\vec{k}-\vec{k}_o, \omega-\omega_o) + \vec{E}_o \cdot \chi_L^{NL}(\vec{k}_o,\omega_o;\vec{k}+\vec{k}_o,\omega+\omega_o) \cdot$$

$$E_L(\vec{k}+\vec{k}_o,\omega+\omega_o) . \tag{2.70}$$

34

Similarly one writes

$$P_L(k,\omega-\omega_o) = -E_L(k,\omega-\omega_o) = E_L(k,\omega-\omega_o)\chi_L(\vec{k},\omega-\omega_o)$$

$$+ E_o \cdot \chi_L^{NL}(-k_o,-\omega_o,\vec{k},\omega)E_L(k,\omega) \tag{2.71}$$

Rewriting Equations 2.70 and 2.71, we get

$$\varepsilon_L(k,\omega)E_L(k,\omega)+\vec{E}_o\cdot\chi_L^{NL}(\vec{k}_o,\omega_o;\vec{k},\omega-\omega_o)E_L(\vec{k},\omega-\omega_o) = 0 \tag{2.72}$$

$$E_o\cdot\chi_L^{NL}(-k_o,-\omega_o,\vec{k},\omega)E_L(k,\omega)+\varepsilon_L(k,\omega-\omega_o)E_L(\vec{k},\omega-\omega_o) = 0 \tag{2.73}$$

where E_L is the effective longitudinal electric field in the plasma, $\varepsilon_L(k,\omega)$ is the linear longitudinal dielectric constant and χ_L is the total susceptibility of the electron ion plasma. χ_L^{NL} is the nonlinear longitudinal susceptibility that connects the longitudinal polarization to $E_L(\omega \pm \omega_o)$.

In writing Equations 2.72 and 2.73, it has been assumed that inside the medium $\vec{k} - \vec{k}_o \approx \vec{k}$ [31].

Now Equations 2.72 and 2.73 will have a non-trivial solution if

$$\varepsilon_L(\vec{k},\omega)-\vec{E}_o\cdot\vec{\chi}_L^{NL}(\vec{k}_o,\omega_o;\vec{k},\omega-\omega_o)\vec{E}_o\cdot\vec{\chi}_L^{NL}(-\vec{k}_o,-\omega_o;\vec{k},\omega)\,[\varepsilon_L(\vec{k},\omega-\omega_o)]^{-1} = 0 \tag{2.74}$$

The left hand side of Equation 2.74 is also called the non-linear longitudinal dielectric constant

$$\varepsilon_L^{NL}(\vec{k},\omega).$$

It can be shown that [32]

$$\vec{E}_o\cdot\vec{\chi}_L^{NL}(\vec{k}_o,\omega_o;\vec{k},\omega-\omega_o) = \left(-\frac{ie\vec{k}\cdot\vec{E}_o}{2m_e\omega_o^2}\right)\left[\chi_L^e(k,\omega-\omega_o)-\chi_L^e(\vec{k},\omega)\right] \tag{2.75}$$

35

If now

$$\frac{k}{k_D} \ll 1,$$

where

$$k_D = \sqrt{\frac{4\pi n e^2}{k_B T}},$$

then the term in the square brackets in Equation 2.75 can be shown to be equal to

$$\sim \frac{k_D^2}{k^2}.$$

$$\therefore \quad \vec{E}_o \cdot \vec{\chi}_L^{NL}(\vec{k}_o,\omega_o;\vec{k},\omega-\omega_o) = - \frac{ie\vec{k}\cdot\vec{E}_o}{2m_e\omega o^2} \frac{k_D^2}{k^2} \qquad (2.76)$$

Substituting this in Equation 2.76,

$$\epsilon_L^{NL}(k,\omega) = \epsilon_L(\vec{k},\omega) - \frac{e^2(\vec{k}\cdot\vec{E}_o)^2}{4m_e^2\omega_o^4}\left(\frac{k_D^2}{k^2}\right)^2 [\epsilon_L(\vec{k},\omega-\omega_o)]^{-1}$$

or

$$\epsilon_L^{NL}(\vec{k},\omega) = \epsilon_L(\vec{k},\omega) - \frac{\Lambda^2}{\left(\frac{k^2}{k_D^2}\right)\epsilon_L(\vec{k},\omega-\omega_o)} \qquad (2.77)$$

where

$$\Lambda^2 = \frac{1}{4}\left(\frac{\omega_p}{\omega_o}\right)^4 \cos^2\theta \frac{I_o}{nck_B T}$$

and I_o is the incident intensity.

Expression 2.77 will be used in Chapter 4 to explain CO_2 damage thresholds.

36

REFERENCES

1. R. A. Smith, Semiconductors (Cambridge at University Press, 1968).

2. E. O. Kane, "Theory of Photoelectric Emission from Semiconductors," Phys. Rev. 127, 131 (1962).

3. G. W. Gobeli and F. G. Allen, "Work Function, Photoelectric Threshold, and Surface States of Atomically cleaned Silicon," Phys. Rev. 127, 150 (1962).

4. J. Bardeen, F. J. Blatt and L. H. Hall, Proceedings of Atlantic City Photoconductivity Conference (1954), p. 146 (John Wiley and Sons and Chapman and Hall, 1956).

5. G. G. MacFarlane, T. P. McLean, J. E. Quarrington and V. Roberts, "Direct Optical Transitions and Further Exciton Effects in Germanium," Proc. Phys. Soc., 71, 863 (1958).

6. G. G. MacFarlane, T. P. McLean, J. E. Quarrington and V. Roberts, "Fine Structure in the Absorption Edge of Ge," Phys. Rev. 108, 1377 (1957).

7. H. Y. Fan, "Infra-Red Absorption in Semiconductors," Rep. Progr. Phys. (London Physical Society) 19, 107 (1956).

8. H. Y. Fan in Semiconductors and Semimetals, Editors R. K. Willardson and A. C. Beer, Vol. 3 (Academic Press, New York and London, 1967) p. 405.

9. A. F. Gibson, "The Absorption of 39 kMc/s (39Gc/s) Radiation in Germanium," Proc. Phys. Soc. B, 69, 488 (1956).

10. F. Urbach, "The Long-Wavelength Edge of Photographic Sensitivity and of the Electronic Absorption in Solids," Phys. Rev. 92, 1324 (1953).

11. R. S. Knox, Theory of Excitons, (Academic Press, New York, 1963).

12. J. D. Dow and D. Redfield, "Theory of Exponential Absorption Edges in Ionic and Covalent Solids," Phys. Rev. Letters 26, 762 (1971).

13. W. Spitzer and H. Y. Fan, "Infrared Absorption in Indium Antimonide," Phys. Rev. 99, 1893 (1955).

14. M. Lax and E. Burstein, "Infrared Lattice Absorption in Ionic and Homopolar Crystals," Phys. Rev., 97, 39 (1955).

15. C. A. Kittel, Introduction to Solid State Physics, 4th Edition (John Wiley, New York 1970), p. 155.

16. M. Bass and H. H. Barret, "Avalanche Breakdown and the Probabilistic Nature of Laser Induced Damage," IEEE J. of Quantum Electronics, QE-8, 3, 343 (1972).

17. E. Yablonovitch and N. Bloembergen, "Avalanche Ionization and the Limiting Diameter of Filaments Induced by Light Pulses in Transparent Media," Phys. Rev. Letters, 29, 907 (1972).

18. R. A. Shatas, J. D. Stettler, L. M. Narducci, S. S. Mitra and H. C. Meyer, Laser Induced Damage in Optical Materials, Editors A. J. Glass and A. H. Guenther, N. B. S. Special Publication 414, Washington, D. C. (1974) p. 200.

19. R. Y. Chio, E. Garmire and C. H. Townes, "Self Trapping of Optical Beams," Phys. Rev. Letters, 13, 479 (1964).

20. P. L. Kelley, "Self Focusing of Optical Beams," Phys. Rev. Letters 15, 1005 (1965).

21. Y. R. Shen and J. H. Marburger in Progress in Quantum Electronics, Vol. 4, Part 1, Editors J. H. Sanders and S. Sten Rolm (Pergamon Press, Oxford, New York 1975).

22. S. A. Akhmanov, A. P. Sukhorukov and R. V. Khokhlore, "Self Focusing and Diffraction of Light in a Nonlinear Medium," Soviet Phys., Uspekhi, 10, 609 (1968).

23. A. Feldman, D. Horovitz and R. M. Waxler, "Mechanisms of Self Focusing in Optical Glasses," IEEE J. of Quantum Electronics, Q.E.9, No. 11, 1054 (1973).

24. A. G. Litvak, "Self Focusing of Powerful Light Beams by Thermal Effects," Soviet Phys., JETP Lett. 4, 250 (1966).

25. E. L. Kerr, "Track Formation in Optical Glass Caused by Electro-strictive Laser Beam Self Focusing," Phys. Rev. A, 4, 1195 (1971).

26. Y. R. Shen, "Electrostriction, Optical Kerr Effect and Self Focusing of Laser Beams," Phys. Rev. Lett., 20, 378 (1966).

27. F. E. Cap, Handbook on Plasma Instabilities, Vol. 1 (Academic Press, New York, San Francisco, London 1976).

28. F. F. Chen, Introduction to Plasma Physics, Plenum Press, New York, London (1974) p. 175.

29. K. Nishikawa, "Parametric Excitation of Coupled Waves II. Parametric Plasmon-Photon Interaction," J. Phys. Soc. Japan, 24, 1152 (1968).

30. P. K. Kaw and J. M. Dawson, "Laser Induced Anomalous Heating of a Plasma," The Phys. of Fluids 12, 2586 (1969).

31. D. F. DuBois and M. V. Goldman, "Radiation Induced Instability of Electron Plasma Oscillations," Phys. Rev. Lett. 14, 544 (1965).

32. D. F. DuBois and M. V. Goldman, "Parametrically Excited Plasma Fluctuations," Phys. Rev. 164, 1, 207 (1967).

33. M. V. Goldman," Parametric Plasmon-Photon Interactions," Ann. of Physics, 38, 117 (1966).

34. D. F. DuBois and M. V. Goldman, "Spectrum and Anomalous Resistivity for the Saturated Parametric Instability," Phys. Rev. Lett., 28, 218 (1972).

35. E. A. Jackson, "Parametric Effects of Radiation on a Plasma," Phys. Rev. 153, 235 (1967).

36. V. P. Silin, "Parametric Resonance in a Plasma," Sov. Phys. JETP, 21, 1127 (1965).

37. R. A. Stern and N. Tzoar, "Parametric Coupling between Electron-Plasma and Ion-Acoustic Oscillations," Phys. Rev. Lett., 17, 903 (1966).

CHAPTER 3

HALL EFFECT AND SCATTERING MECHANISMS

Since its discovery in 1879 [1], Hall effect has been one of the most powerful methods for determining the carrier mobility and carrier concentration in semiconductors. Till recently, this method had the disadvantage of requiring devices of specific shape. But in 1958, Van der Pauw [2] extended this method to be applied to a sample of any shape. In the following, we shall give the theory of Hall effect and Van der Pauw's method and describe the experimental details of determining mobility and carrier concentration, before and after laser damage.

1. HALL EFFECT [3]

When a conductor or a semiconductor carrying current is placed in a magnetic field, an electromotive force is produced across it in a direction perpendicular to both the current and the magnetic field. This is called Hall effect.

Consider an n-type semiconductor bar of infinite length and width d, as shown in Figure 3-1. Let $\vec{j}$ be the current density in the x direction and a magnetic field $\vec{H}$ be applied in the z-direction. Let n be the carrier density.

The Lorentz force on an electron in the bar is given by

$$\vec{F} = e[\vec{E} + (\vec{v} \times \vec{H})]$$ (3.1)

where $\vec{E}$ is the electric field and $\vec{v}$ is the velocity of the electron.

As no current can flow in the y-direction, the net Lorentz force in this direction must be zero,
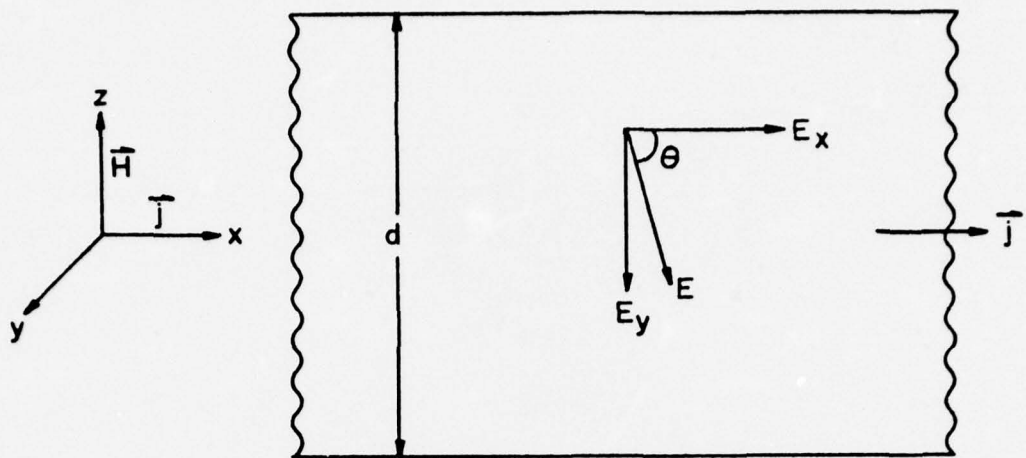
Figure 3-1. A current carrying semiconductor bar
of infinite length placed in a
magnetic field

i.e.,

$$F_y = 0$$

or

$$e[E_y + (\vec{v} \times \vec{H})_y] = 0$$

or

$$E_y + v \cdot H = 0$$

i.e.,

$$E_y = -H \cdot v \qquad\qquad (3.2)$$

But

$$|\vec{j}| = ne|\vec{v}|$$

$$\therefore \quad \vec{E}_y = -\frac{H\vec{j}}{ne} \qquad\qquad (3.3)$$

Equation 3.3 gives the magnitude of the Hall field. Now an

electronic flow in the x-direction sets up an electric field,

given by

$$\vec{j} = \sigma \vec{E}_x \tag{3.4}$$

where σ is the electrical conductivity of the semiconductor,

or

$$\vec{j} = ne\mu_e \vec{E}_x \tag{3.5}$$

From Equations 3.3 and 3.5,

$$\frac{|E_y|}{|E_x|} = \tan\theta = -H\mu_e \tag{3.6}$$

where θ is called the Hall angle.

Equation 3.3 is usually written as

$$|\vec{E}_y| = RH\vec{j} \tag{3.7}$$

where

$R = -\dfrac{1}{ne}$, and is called Hall constant. In deriving the

above equation, one has to assume that the energy surfaces of the

semiconductor are spherical, which is rarely true. Therefore, the

expression for the Hall constant should be corrected as

$$R = -\frac{r}{ne} \tag{3.8}$$

where r now would depend upon the type of energy surface involved.

In general, it can be shown [3] that

$$R = -\frac{1}{ne} \frac{(\overline{\tau}_e)^2}{\overline{\tau_e^2}} \tag{3.9}$$

where $\overline{\tau}_e$ represents the statistical average of the electron life-

time over the proper distribution function.

42

If $\tau_e \propto E^{-\frac{1}{2}}$, which is true in acoustic phonon lattice scattering (E being the energy), then

$$\frac{(\overline{\tau_e})^2}{\overline{\tau_e^2}} = \frac{3\pi}{8}$$

so that

$$R = -\frac{1}{ne} \cdot \frac{3\pi}{8} \tag{3.10}$$

If $\tau_e \propto E^{3/2}$ as in case of ionized impurity scattering, then [4],

$$\frac{(\overline{\tau_e})^2}{\overline{\tau_e^2}} = \frac{315}{512}\pi$$

$$\therefore \quad R = -\frac{1}{ne}\left(\frac{315\pi}{512}\right) \tag{3.11}$$

From Equations 3.10 and 3.11 it can be seen that in practice r is very close to unity and can be considered so in experimental measurements.

The conductivity of an n-type sample may be written as

$$\sigma = -ne\mu_c \tag{3.12}$$

where μ_c is called conductivity mobility.

Substituting for ne in Equation 3.8, one gets

$$R = r \cdot \frac{\mu_c}{\sigma}$$

or $\quad \mu_c = R\frac{\sigma}{r} = \frac{\mu_H}{r} \tag{3.13}$

where $\mu_H = R\sigma$ and is called <u>Hall mobility</u>. When $r = 1$,

$$\mu_c = \mu_H .$$

43

If in a sample both the holes and electrons are present, then it can be shown [5] that

$$R = \frac{1}{e} \frac{p\mu_h^2 - n\mu_e^2}{(p\mu_h + n\mu_e)^2} \tag{3.14}$$

A determination of R experimentally determines the carrier concentration in a sample. If the conductivity is known, then one can also determine the mobility of the carriers. As stated in the beginning, this method requires a sample which is effectively very long as compared to its width. Van der Pauw has extended Hall effect method in such a way that it can be applied to a sample of an arbitrary shape.

2.   VAN DER PAUW METHOD [2]

Consider a sample of an arbitrary shape as shown in Figure 3-2. Let d be its thickness and let A, B, C and D be four ohmic contacts on the periphery of the sample.
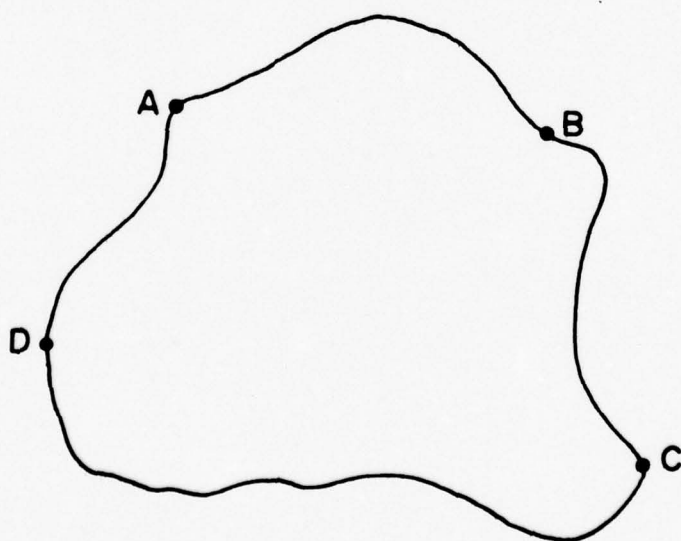
Figure 3-2.   A sample of arbitrary shape

44

Assume the following:

(a)   The contacts are at the circumference of the sample.

(b)   The contacts are sufficiently small.

(c)   The sample is homogeneous in thickness.

(d)   The surface of the sample is singly connected and
      has no isolated regions.

Define

$$R_{AB,CD} = \frac{V_C - V_D}{I_{AB}} ,$$

then one can show by using elementary electrostatics that

$$\exp\left[-\pi R_{AB,CD}\frac{d}{\rho}\right] + \exp\left[-\pi R_{BC,DA}\frac{d}{\rho}\right] = 1 \qquad (3.15)$$

Here ρ is the specific resistance of the sample. Solving Equation 3.15 for ρ,

$$\rho = \frac{\pi d}{\ell n 2}\frac{(R_{AB,CD} + R_{BC,DA})}{2}\; f\left[\frac{R_{AB,CD}}{R_{BC,DA}}\right] \qquad (3.16)$$

where f is a function of the ratio

$\dfrac{R_{AB,CD}}{R_{BC,DA}}$ only and satisfies

$$\frac{R_{AB,CD} - R_{BC,DA}}{R_{AB,CD} + R_{BC,DA}} = f\ \mathrm{arc\ cosh}\left|\frac{\exp(\ell n\ 2/f)}{2}\right| .$$

If $R_{AB,CD}$ and $R_{BC,DA}$ are nearly equal (which will be true for a sample of nearly square shape), f can be approximated by

$$f \cong 1 - \left[\frac{R_{AB,CD} - R_{BC,DA}}{R_{AB,CD} + R_{BC,DA}}\right]^2 \frac{\ell n 2}{2}$$

$$- \left[\frac{R_{AB,CD} - R_{BC,DA}}{R_{AB,CD} + R_{BC,DA}}\right]^4 \left|\frac{(\ell n 2)^2}{4} - \frac{(\ell n 2)^3}{12}\right|$$

45

If $R_{AB,CD}$ and $R_{BC,DA}$ are exactly equal, then

$$f = 1,$$

and from Equation 3.16

$$\rho = \frac{\pi d}{\ln 2} R_{AB,CD} \qquad (3.17)$$

Now if a magnetic field is applied perpendicular to the sample, then the equations

$$\text{div } \vec{j} = 0$$

$$\text{curl } \vec{j} = 0$$

where $\vec{j}$ is the current density, remain valid. As the contacts are sufficiently small and at the circumference of the sample, the outer lines of flow which must follow the circumference fully determine our boundary conditions. Hence the lines of flow do not change when a magnetic field is applied. However, the magnetic field causes an extra potential difference between any two arbitrary points. This can be shown from Hall effect to be

$$\Delta V = \frac{\mu_H H I \rho}{d} -$$

where μ_H is the Hall mobility and I is the current.

$$\therefore \quad \mu_H = \frac{d}{\rho H} \frac{\Delta V}{I}$$

$$\text{or} \quad \mu_H = \frac{d}{\rho H} \Delta R_{BC,AC} \qquad (3.18)$$

where H is the magnetic field and $\Delta R_{BD,AC}$ is the change of $R_{BD,AC}$ due to the magnetic field.

Using Equations 3.17 and 3.18, one can find the resistivity and Hall mobility of a sample, provided one has

(a) A square sample of the semiconductor

(b) Four ohmic contacts on the four corners of the sample.

46

3.   FABRICATION OF HALL DEVICE

Bulk semiconductor materials Si, Ge, GaAs and GaP were obtained commercially in wafers ranging from 0.01 cm to 0.025 cm in thickness. $GaAs_xP_{1-x}$ was obtained in epitaxial ($\sim$300 μm) wafer form on intrinsic (10^8 Ωcm) GaAs substrate.

These wafers were lapped, polished and chemically cleaned, using procedures developed at The University of New Mexico.   A description of these procedures is given elsewhere [6].

Ohmic contacts were evaporated on these wafers through specially prepared masks in a vacuum evaporation system at pressures of 10^{-6} torr.   These contacts were heat treated in an inert atmosphere from 5 to 15 minutes.   The current-voltage characteristics between any two contacts showed good ohmic contacts.

A diamond subscriber was used to cut the wafers into (.25 x .25) cm^2 Hall devices.   The Hall device was mounted on heat conducting alumina plates by using heat conducting, electrically insulating epoxy.   Four strips of aluminum were evaporated on the four corners of the alumina substrate.   Wire bonds were made between these four plates and the four ohmic contacts on the sample. A typical Hall effect device is shown in Figure 3-3.
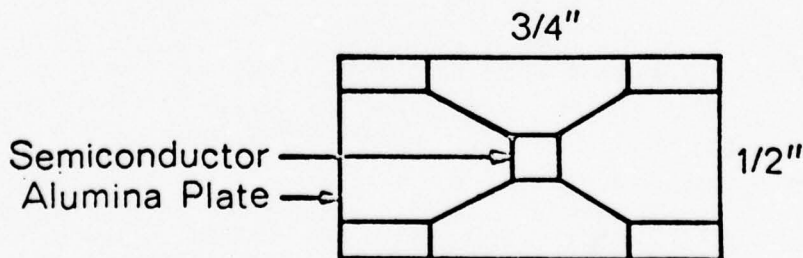
Figure 3-3.   A Hall effect device

47

4.   DESCRIPTION OF MOBILITY APPARATUS

The Hall effect device shown in Figure 3-3 was mounted on a stage specially prepared from high quality oxygen free copper. This stage was placed in perfect thermal contact at the cold tip of the displacer of a cryogenic refrigerator, as shown in Figure 3-4.

The displacer is surrounded by a vacuum shroud that is evacuated to 10^{-4} torr by using a mechanical-diffusion pump system. Four wires are fed through to make electrical connections to the Hall device. A heater element is wound over the cold tip to control its temperature, which can be adjusted from 12°K to 300°K. A chromel vs. gold--0.07 atomic percent iron thermocouple is used to measure the temperature of the cold end to an accuracy of ±0.2%.

The displacer assembly is mounted between adjustable pole pieces of a water cooled electromagnet. The magnet is capable of giving fields up to 2.5 teslas.

Resistivity and mobility were determined using the following steps.

Step 1: A current of a few milliamperes was passed through two adjacent contacts of the sample by using dc batteries. The Hall induced electromotive force was measured across the other two contacts. The current was then reversed in direction and Hall voltage was remeasured. This was repeated for all combinations of adjacent contacts and the average of the eight readings was taken to give $R_{AB,CD}$ of Equation 3.17 and hence to determine resistivity ρ.

Step 2: The current is now passed through two diagonal con-

48
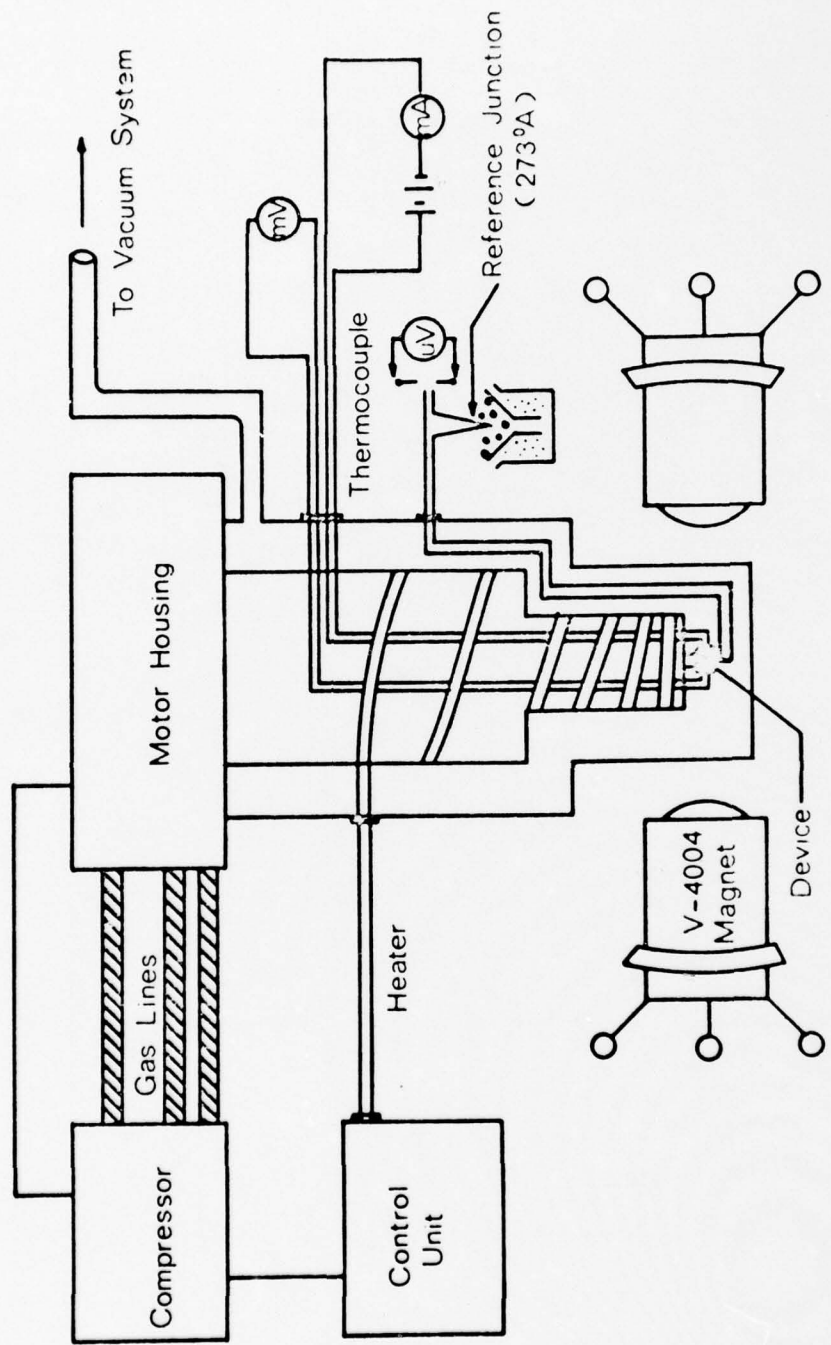
Figure 3-4.   Mobility and resistivity apparatus

49

tacts of the sample and the Hall voltage is measured across the other two diagonal contacts. Then a magnetic field is applied in a direction perpendicular to the direction of current and the change in Hall voltage determined. The magnetic field is reversed and the change in Hall voltage remeasured.

Step 3: The current through the device is reversed and Step 2 is repeated.

Step 4: The current is now passed through the other two diagonal contacts and Steps 2 and 3 are followed.

Average of these eight readings is taken to give $\Delta R_{BD,AC}$ of Equation 3.18 and thus Hall mobility is determined.

5. SCATTERING MECHANISMS

The mobility of carriers in a semiconductor is determined by the scattering mechanisms in the lattice. Radiation damages the lattice structure of semiconductors due to which electronic properties are degraded. Particle damage is known to cause change in carrier concentration, lifetime and mobility of a semiconductor due to the creation of interstitial-vacancy pairs or complexes. These changes may be significant depending on the amount of radiation dose. The defects introduced may or may not dominate the electrical properties at room temperature because of the lattice vibrations. However, at low temperatures lattice vibrations can be killed and the effect of the introduced defects easily observed. Therefore, in this chapter the temperature dependence of different scattering mechanisms that control the carrier mobility and electrical conductivity of the semiconductor lattice

50

will be examined. This dependence is what eventually determines the nature of radiation induced defects.

Scattering mechanisms can be divided into three parts.

(a) Lattice scattering [7, 8, 9]

(b) Impurity scattering: ionized [10, 11] and un-ionized [12]

(c) Defects [13, 14], intervalley [15] and carrier-carrier scattering [16]

(a) Lattice Scattering

The vibration spectrum of semiconductors has two branches, namely optical and acoustical. At moderate and low temperature, the thermal energy available is insufficient to excite the high frequency optical mode and, therefore, the scattering of carriers can be due to acoustical vibrations only. One considers only the scattering of charged carriers by longitudinal mode vibrations, because the effect of transverse modes can be shown to be negligible.

The passage of a longitudinal vibration through a crystal would give rise to alternate regions of compression and extension. A compressed region would exhibit an increase in band gap, while an extension would cause a decrease in the band gap. This is shown in Figure 3-5.

Along the length of the crystal, therefore, the band gap as a function of distance would look like that shown in Figure 3-6(a) and can be approximated by Figure 3-6(b). One may then calculate the reflection probability for an electron incident upon a single step of height δE_c as shown in Figure 3-6(b). Neglecting Doppler effect due to a barrier moving at the speed of sound, it can be shown from elementary quantum mechanics that

51
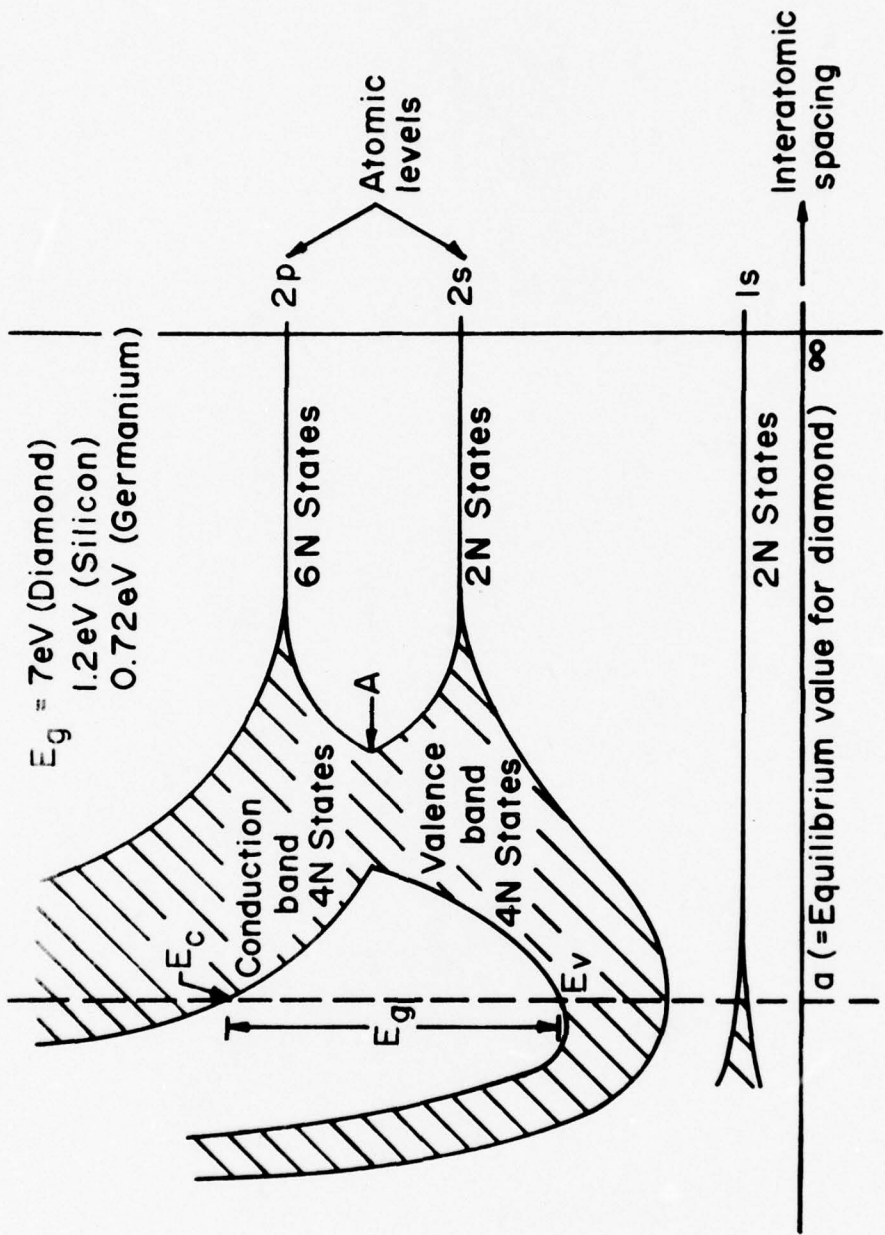
Figure 3-5. The bands arising from the 1s, 2s, 2p atomic states of carbon (diamond) as a function of interatomic distance (after Reference [17])
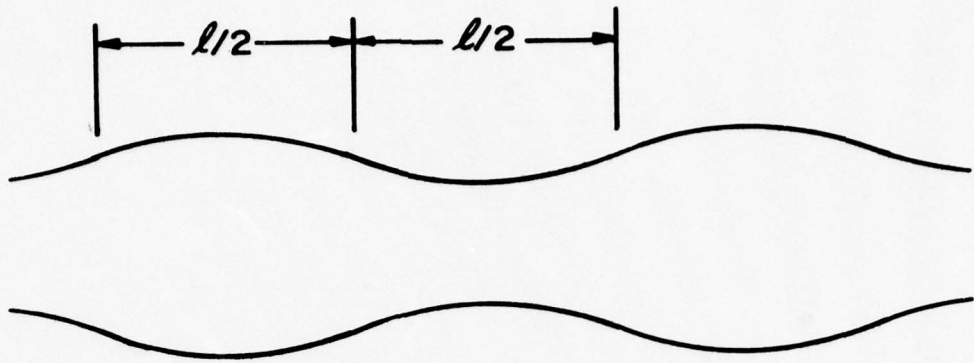
Figure 3-6(a). The sinusoidal variation of band gap caused by the compressional and extensional forces associated with longitudinal thermal vibration
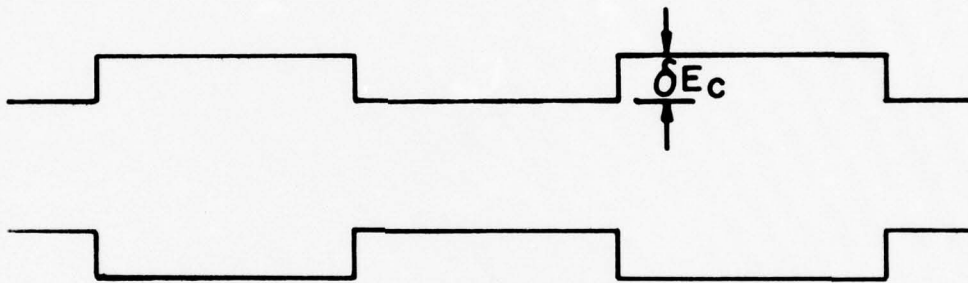
Figure 3-6(b). A "square wave" variation which approximates the one shown in Figure 3-6(a)

$$R = \left(\frac{k_o - k_1}{k_o - k_1} \right)^2 \tag{3.19}$$

$$\text{and} \quad T = \frac{4 k_o k_1}{(k_o + k_1)^2} \tag{3.20}$$

where

$$k_o = \sqrt{\frac{2 m^*_e E_o}{\hbar^2}} \tag{3.21}$$

$$\text{and} \quad k_1 = \sqrt{\frac{2 m^*_e (E_o - \delta E_c)}{\hbar^2}}$$

E_o being the energy of the incident electron. If the step δE_c is small, which can safely be assumed, then $k_1 \cong k_o$. With this approximation, Equation 3.19 becomes

$$R \cong \left(\frac{m^*_e \delta E_c}{2\hbar^2 k^2}\right) \tag{3.22}$$

Now to a first approximation

$$\delta E_c = - \eta' \left(\frac{\delta V}{V_o}\right) \tag{3.23}$$

where

$$\frac{\delta V}{V_o}$$

represents compressional or extensional strain and η' is the deformation potential constant. If δp is the maximum pressure created by the compression or extension, then the stored strain energy is

$$\delta E = \frac{1}{2} \delta p \delta V = \lambda' k_B T \tag{3.24}$$

where λ' is a constant. The term $\lambda' k_B T$ arises because the source of this strain energy is thermal. Also by definition the bulk compressibility is given as

$$\beta = \frac{1}{V_o} \frac{\delta V}{\delta p} \tag{3.25}$$

From Equations 3.24 and 3.25, one has

$$\left(\frac{\delta V}{V_o}\right)^2 = \frac{2\beta \lambda' k_B T}{V_o} \tag{3.26}$$

Substituting this in Equation 3.23 gives

$$\delta E_c \cong -\eta' \sqrt{\frac{2\beta \lambda' k_B T}{V_o}} \tag{3.27}$$

54

From Equations 3.22 and 3.27 one has

$$R \cong \frac{m_e^{*2} \eta^2 \beta \lambda' k_B T}{2 V_o (\hbar^4 k_o^4)} \qquad (3.28)$$

If $\ell/2$ is the linear dimension of the volume V_o, λ_e the mean free path, then in going through a distance $\ell/2$, the scattering probability is $\ell/2\lambda_e$. Therefore, replacing R in Equation 3.28 by $\ell/2\lambda_e$ produces

$$\frac{\ell}{2\lambda_e} = \frac{m_e^{*2} \eta'^2 \beta \lambda' k_B T}{V_o (\hbar^4 k_o^4)}$$

or

$$\lambda_e = \frac{h^4}{8 m_e^{*2} \lambda' \beta k_B T \eta'^2} \qquad (3.29)$$

where we have replaced k_o by $2\pi/\ell$ and V_o by $\ell^3/8$.

The collisions between electrons and phonons are very similar to perfectly elastic collisions between two hard spheres and can be described by a velocity independent mean free path. Assuming the velocity distribution of electrons is Maxwell Boltzmann it can be easily shown that the mean free time $\bar{\tau}_e$ is given by [18]

$$\bar{\tau}_e = \frac{8\lambda_e}{3\pi\bar{c}} \qquad (3.30)$$

where $\bar{c}$ is the mean thermal speed of the electron. From Equations 3.29 and 3.30 one has

$$\bar{\tau}_e = \frac{h^4}{3\sqrt{8\pi} \; m_e^{*3/2} \lambda' \beta (k_B T)^{3/2} \eta'^2} \qquad (3.31)$$

Even though the above equation has been derived qualitatively,

55

it is not very much different from the quantum-mechanical expression [19], which is given as

$$\tau_e = \frac{\sqrt{8}}{3} \frac{\hbar^4 C_{\ell\ell}}{m_e^{*3/2} (k_B T)^{3/2} \eta'^2}$$ (3.32)

where $C_{\ell\ell}$ is the elastic constant for a longitudinal extension in the [110] direction. The corresponding mobility is

$$\mu_e = \frac{e\bar{\tau}_e}{m_e^*} = \frac{\sqrt{8}}{3} \frac{e\hbar^4 C_{\ell\ell}}{m_e^{*5/2} (k_B T)^{3/2} \eta'^2}$$ (3.33)

The theoretical prediction $\mu_e \propto T^{-3/2}$ is only approximately true and in actual practice the variation is found to be stronger in Ge and Si. This can be attributed to the following reasons.

(i)   In p-type Ge and Si, optical scattering cannot be ignored.

(ii) In n-type Ge and Si, energy surfaces are ellipsoidal and effects of multivalley scattering cannot be ignored [20].

(b)   Impurity Scattering

Ionized Impurities. The determination of the effect of ionized impurity scattering on mobility of electrons is based on the theory of scattering of charged particles by the coulomb potential of the nucleus, which was originally developed by Rutherford [21]. He showed that the scattering cross section of a charged particle of charge e by a fixed nucleus of charge Ze is given by

56

$$\sigma(\theta)\,d\Omega = \left(\frac{Ze^2}{2\epsilon m_e^* v_o^2}\right)\frac{1}{\sin^4\frac{\theta}{2}}\,d\Omega \qquad (3.34)$$

where

$$\tan\frac{\theta}{2} = \frac{Ze^2}{\epsilon a m_e^* v_o^2} \qquad (3.35)$$

The meanings of the various terms involved in Equations 3.34 and 3.35 can be seen from Figure 3-7.
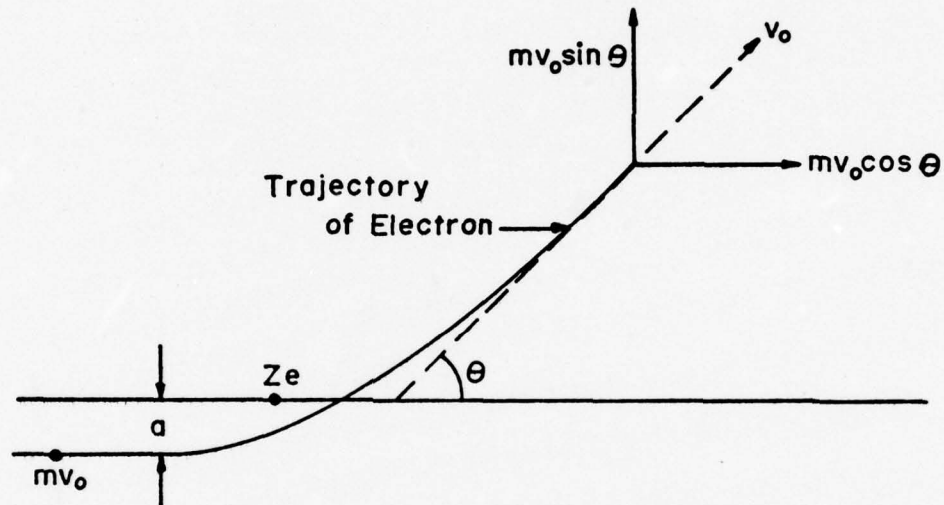
Figure 3-7. Rutherford scattering of an electron from a nucleus of charge Ze

The number of collisions an electron can make per unit time into a solid angle $d\Omega$ can be shown to be $Nv_o\sigma(\theta)\,d\Omega$ where N is the number of charged scattering centers per unit volume. In each such collision the momentum change is only $mv_o(1 - \cos\theta)$, as can be seen from Figure 3-7. The relaxation time, however, is the time during which the average forward momentum is zero. Hence in

57

this sense, the effective number of collisions is given by

$$dn_{eff} = Nv_o\sigma(\theta)(1 - \cos\theta)d\Omega = d\left(\frac{1}{\tau_e}\right) \tag{3.36}$$

Equation 3.36 gives the differential of inverse time period for electrons of initial velocity v_o scattered through an angle θ into a solid angle $d\Omega$. The total relaxation time may be found by integrating Equation 3.36 over the solid angle and averaging over velocities.

Assuming the scattering to be independent of the azimuthal angle, integration of Equation 3.36 over the solid angle from polar angle θ_o to π gives

$$\frac{1}{\tau(v_o)} = 2\pi Nv_o \int_{\theta_o}^{\pi} \sigma(\theta)(1 - \cos\theta)\sin\theta d\theta$$

$$= 8\pi Nv_o \left(\frac{Ze^2}{2\epsilon m^* v_o^2}\right)^2 \ln\left[1 + \left(\frac{\epsilon m^* v_o^2}{2Ze^2 N^{1/3}}\right)\right] \tag{3.37}$$

The lower limit of integration has not been taken to be zero, because in a crystal the coulomb potential of an ion has to be cut off at a certain distance from it due to the presence of other ions. It is reasonable to take this distance to be $d/2$ where $d = N^{-1/3}$ is the mean distance between impurity atoms.

$$\therefore \quad a = \frac{1}{2N^{1/3}}$$

and accordingly,

$$\theta = \theta_o = 2\tan^{-1}\left(\frac{2Ze^2 N^{1/3}}{\epsilon m^* v_o^2}\right)$$

58

This expression has already been used to get Equation 3.37.

It is now necessary to average Equation 3.37 over the Max-wellian distribution of velocities.

$$\bar{\tau}_e = \frac{\langle v_o^2 \tau(v_o) \rangle}{\langle v_o^2 \rangle}$$

or

$$\bar{\tau}_e = \frac{\varepsilon^3 m_e^{*2}}{2\pi Z^2 e^4 N} \frac{\displaystyle\int_o^\infty \frac{v_o^7 e^{-m_e^* v_o^2/2k_B T} \, dv_o}{\ln\left[1 + \left(\varepsilon m_e^{*2} v_o^2/2Ze^2 N^{1/3}\right)^2\right]}}{\displaystyle\int_o^\infty v_o^4 e^{-m^* v_o^2/2k_B T} \, dv_o} \tag{3.38}$$

The integral in Equation 3.38 can be solved only approximately. This is done by assuming that the logarithmic term varies much more slowly with v_o as compared to the v_o^7 term. Making this approxi-mation

$$\bar{\tau}_e = \frac{8\varepsilon^2 (k_B T)^{3/2} (2m_e^*)^{1/2}}{N \cdot \pi^{3/2} Z^2 e^4 \, \ln\left[1 + \left(7\varepsilon k_B T/2Ze^2 N^{1/3}\right)^2\right]}$$

and hence

$$\mu_e = \frac{e\bar{\tau}_e}{m_e^*} = \frac{8\sqrt{2}\,\varepsilon^2 (k_B T)^{3/2}}{N \cdot \pi^{3/2} Z^2 e^3 m_e^{*1/2} \ln\left[1 + \left(7\,k_B T/2Ze^2 N^{1/3}\right)^2\right]} \tag{3.39}$$

This formula is called Conwell-Weiskopf formula [10]. Equa-tion 3.39 shows that the mobility due to ionized impurity scatter-ing is directly proportional to $T^{3/2}$ and inversely proportional to impurity concentration. Therefore, for low impurity concentrations, only lattice scattering will be dominant.

59

Neutral Impurities. The scattering by neutral impurities is analogous to the scattering of electrons by hydrogen atoms. Erginsoy [12] has shown that the relaxation time for this process is given by

$$\frac{1}{\tau_e} = \left(\frac{20\hbar^3 \epsilon}{e^2 m_e^{*2}}\right) N_n, \text{ where } N_n \text{ is the number of neutral impurities.}$$

Hence mobility dependence due to un-ionized impurities is given by

$$\mu_e = \frac{e\tau_e}{m_e^*} = \frac{e^3 m_e^{*2}}{20\hbar^3 \epsilon N_n}. \tag{3.40}$$

This type of scattering is important only at very low temperatures where most of the impurities are un-ionized.

(c) Defect Scattering, Intervalley Scattering and Carrier-Carrier Scattering

Defects such as dislocations scatter carriers as a result of the strain around the dislocation which gives rise to a deformation potential. This has been treated by Dexter and Seitz [13]. The predicted temperature dependence of the mobility arising from such dislocations is linear in T.

Dislocations also act as acceptors and, therefore, act as negatively charged centers causing additional scattering.

Intervalley scattering involves the inelastic transfer of an electron from one band at a certain crystal momentum to the part of the same band at a different crystal momentum. This has been further discussed by C. Herring [15].

Carrier-carrier scattering can be neglected under ordinary

60

circumstances. However, carrier-carrier collisions randomize the electron velocity distribution, thereby changing the probability of electron scattering through other mechanisms. Such a treatment has been given by Spitzer and Harm [16].

REFERENCES

1. E. H. Hall, "Action of the Magnet on Electric Currents," The Philosophical Magazine, Vol. 9 and 10 (1880) (Reprinted by Beckman Instruments, Inc., Helipot Division, Fullerton, California).

2. L. J. Van der Pauw, "A Method of Measuring Specific Resistivity and Hall Effect of Discs of Arbitrary Shape," Philips Research Reports, 13 (1958).

3. R. A. Smith, Semiconductors (Cambridge University Press, 1968) p. 100.

4. F. J. Blatt, "Theory of Mobility of Electrons," Solid State Physics (Editors F. Seitz and D. Turnbull) 4, 200 (1957).

5. J. P. McKelvey, Solid State and Semiconductor Physics, (Harper & Row, Publishers, New York 1966) p. 288.

6. W. W. Grannemann, et al.,"A Radiation Effects Research Program," Bureau of Engineering Research Report No. EE-192 (71) ONR-005, The University of New Mexico (September 1971).

7. J. Bardeen and W. Shockley, "Deformation Potentials and Mobilities in Non-Polar Crystals," Phys. Rev. 80, 72 (1950).

8. R. K. Willardson and A. C. Beer (Editors), Semiconductors and Semimetals (Transport Phenomenon), Vol. 10 (1975) (Academic Press, New York & London).

9. E. M. Conwell, High Field Transport in Semiconductors, (Academic Press, New York 1967).

10. E. M. Conwell and V. F. Weisskopf, "Theory of Impurity Scattering in Semiconductors," Phys. Rev. 77, 388 (1950).

11. W. Shockley, Electrons and Holes in Semiconductors, (D. Van Nostrand Company, Inc. 1950) p. 539.

12. C. Erginsoy, "Neutral Impurity Scattering in Semiconductors," Phys. Rev., 79, 1013 (1950).

13. D. L. Dexter and F. Seitz, "Effects of Dislocations on Mobility in Semiconductors," Phys. Rev. 86, 964 (1952).

14. G. L. Pearson, W. T. Read and F. J. Mosin, "Dislocations in Plastically Deformed Germanium," Phys. Rev. 93, 666 (1954).

15. C. Herring, "Transport Properties of Many-Valley Semiconductors," Bell Syst. Tech. J. 34, 237 (1955).

16. L. Spitzer, Jr., and R. Harm, "Transport Phenomenon in a Completely Ionized Gas," Phys. Rev. 89, 977 (1953).

17. G. E. Kimball, "The Electronic Structure of Diamond," J. Chem. Phys. 3, 560 (1935).

18. E. H. Putley, The Hall Effect and Related Phenomenon, (Butterworth & Co., Ltd., London 1960).

19. H. Y. Fan, "Temperature Dependence of Energy Gap in Semiconductors," Phys. Rev. 82, 900 (1951).

20. W. P. Dumke, "Deformation Potential Theory for n-Type Ge," Phys. Rev. 101, 531 (1956).

21. E. Rutherford, "The Scattering of α and β Particles by Matter and the Structure of the Atom," Phil. Mag., 21, 669 (1911).

CHAPTER 4

RESULTS: CW CO_2 LASER DAMAGE

The experimental results on damage thresholds and the changes
in electrical properties of the semiconductors due to CO_2 laser
radiation are given in this chapter. The results obtained are
explained theoretically.

The damage thresholds were obtained by radiating the chemi-
cally cleaned semiconductor samples in the form of Hall devices.
The damage criteria used have been described in Chapter 2. The
CW CO_2 laser beam used was Gaussian in space with a diameter of
12 mm. A salt lens of 25 cm focal length was used to concentrate
the beam on the sample. The sample was displaced from the focus
so that the whole area could be uniformly radiated. The experi-
mental arrangement is shown in Figure 4-1.

The absorption coefficients [1] for most semiconductors at
10.6 µm are very small and, therefore, it can be assumed that the
energy is absorbed by the bulk uniformly.

1.   DAMAGE THRESHOLDS

The experimentally observed damage thresholds for different
semiconductors are listed in Table 4-1. Also given in the same
table are their pre-damage mobility, carrier concentration and
band gap.

From this table we observe that the damage thresholds are
all of the same order and are quite insensitive to the original
carrier concentration and mobility.
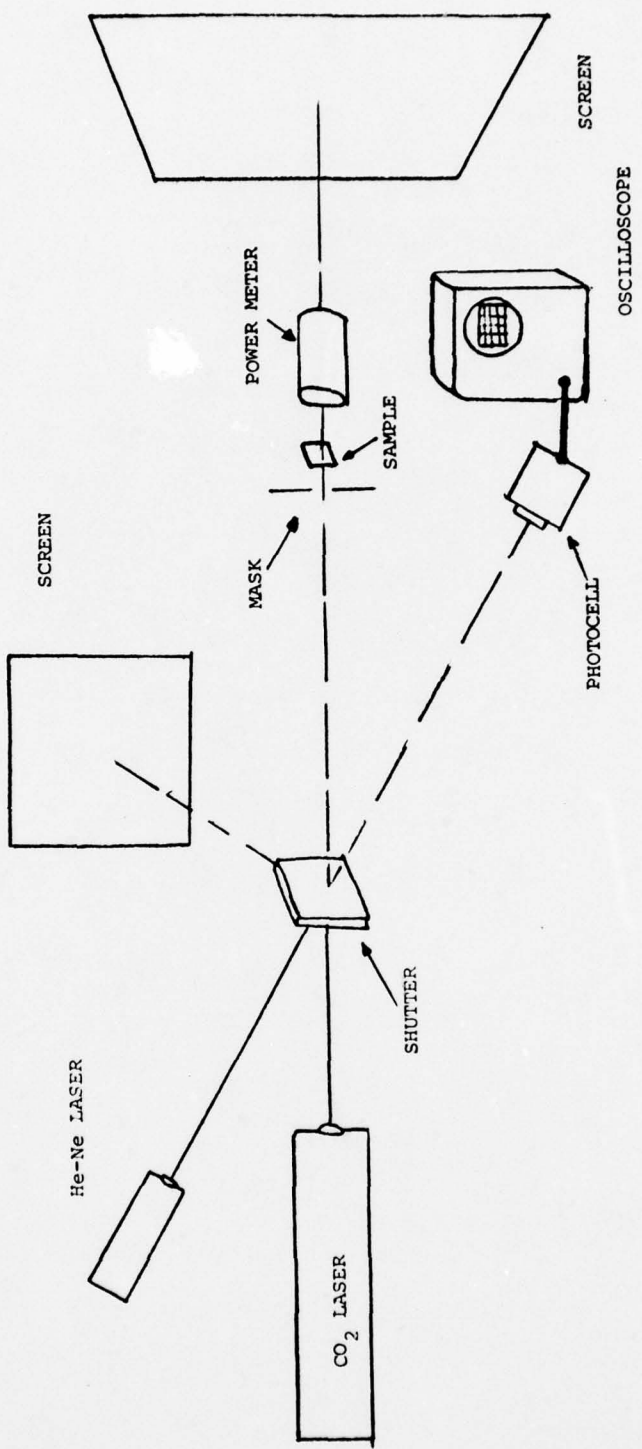
Figure 4-1. Experimental arrangement used to radiate the sample

SCREEN

OSCILLOSCOPE

POWER METER

SAMPLE

MASK

SCREEN

PHOTOCELL

SHUTTER

He-Ne LASER

CO$_2$ LASER

65

Table 4-1. Damage thresholds of different semiconductors

Semiconductor	Mobility $cm^2(V\text{-}sec)^{-1}$	Carrier concentration (cm^{-3})	Band gap (ev)	Damage threshold in $W\ cm^{-2}$
Ge (n-type)	2300	4×10^{14}	0.79	8.5×10^3
Si (n-type)	1200	6×10^{14}	1.11	1.1×10^4
Si (p-type)	300	3×10^{15}	1.11	2.2×10^4
GaAs (n-type)	3500	1×10^{16}	1.40	6×10^3
GaAsP (n-type)	2000	2×10^{17}	2.00	3.5×10^3
GaP (n-type)	110	1×10^{18}	2.4	1.33×10^3

2. ELECTRICAL PROPERTIES

Conductivity

The electrical conductivity of Ge as a function of temperature before and after laser damage is shown in Figure 4-2. It is seen that there is a significant decrease in conductivity due to laser damage, particularly at low temperatures. This shows that the defects introduced by damage are very effective scattering centers at lower temperatures. The lattice vibrations dominate the created defects at room temperature.

Carrier Concentration

The carrier concentration versus temperature before and after laser damage is plotted for Si and Ge in Figures 4-3 and 4-4 respectively. A magnified view of Figure 4-3 is given in Figure 4-5 to show the significant carrier removal due to laser damage.

In general, the carrier concentration is decreased both in Ge and Si at all temperatures. This shows that the laser created scattering centers give rise to localized energy levels in the forbidden band which act as carrier traps.

Mobility

The mobility changes due to laser damage were very small at room temperature. However, as the temperature is lowered, a significant degradation of mobility occurs both in Ge and Si (see Figures 4-6 and 4-7).

This confirms the idea that the introduced defects are more effective scattering centers at lower temperatures.

67
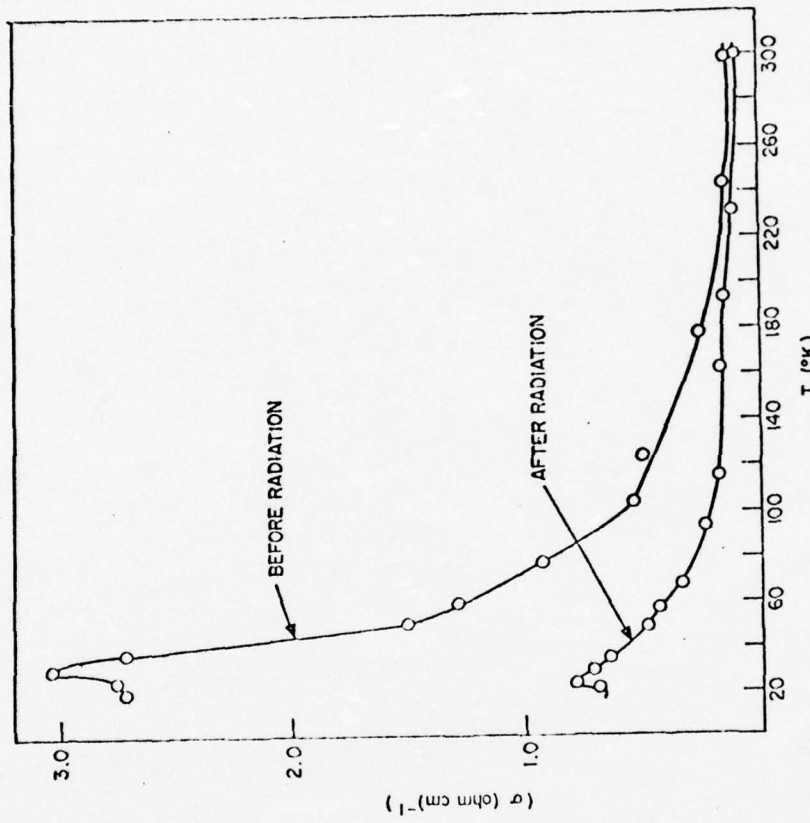
Figure 4-2. Conductivity versus temperature for Ge before and after laser damage (The sample was radiated at 8.3×10^3 W/cm^2. The original carrier concentration was $\sim 10^{14}$cm^{-3}.)

BEFORE RADIATION

AFTER RADIATION

σ (ohm cm)$^{-1}$

T (°K)

Carrier Concentration (cm⁻³)

10^{15}

10^{14}

10^{13}

○ Theoretical

☐ Experimental Points
Before Damage

△ Experimental Points
After Damage

0   40   80   120 160 200 240 280 320

T (°K)
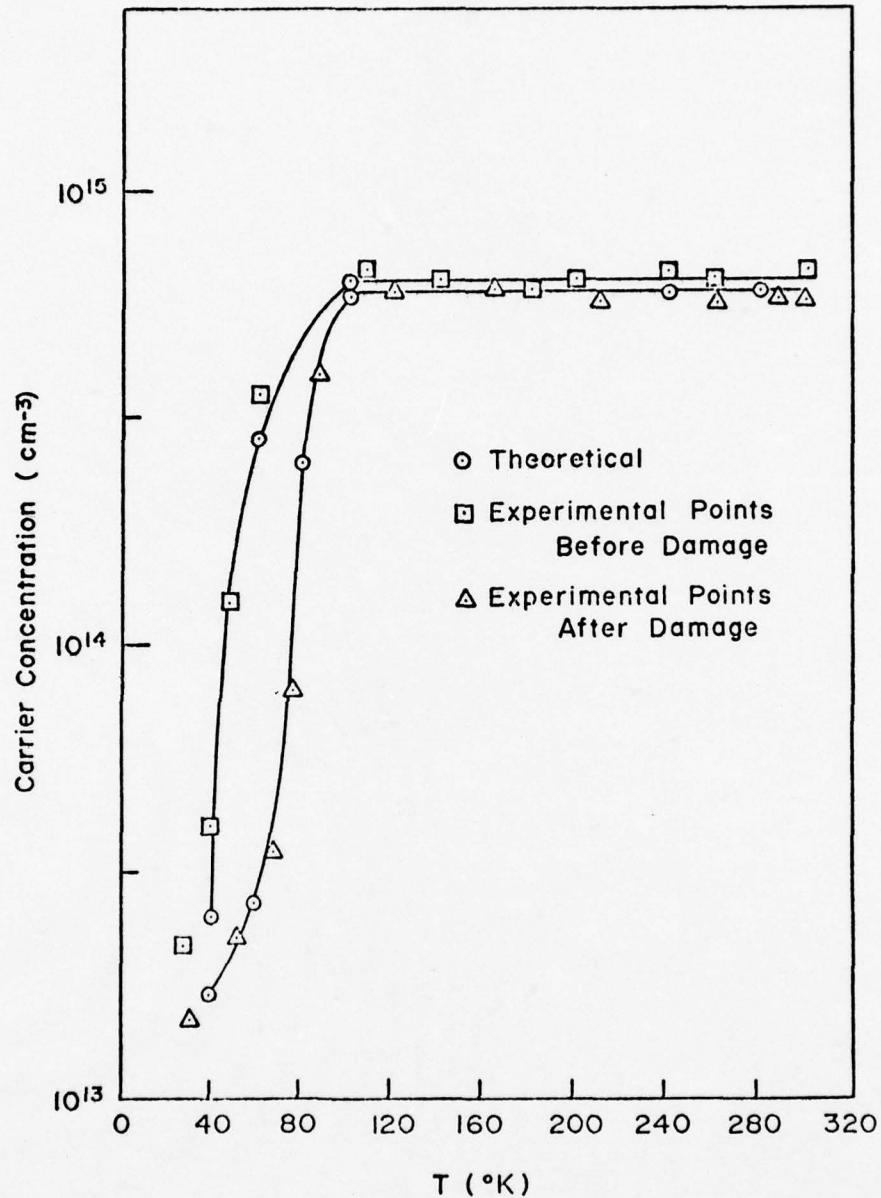
Figure 4-3. Carrier concentration versus temperature for Si be-
fore and after laser damage (The sample was radiated
at 0.96 x 10⁴ watts/cm². The original carrier con-
centration was ~10¹⁵ at room temperature.)

69
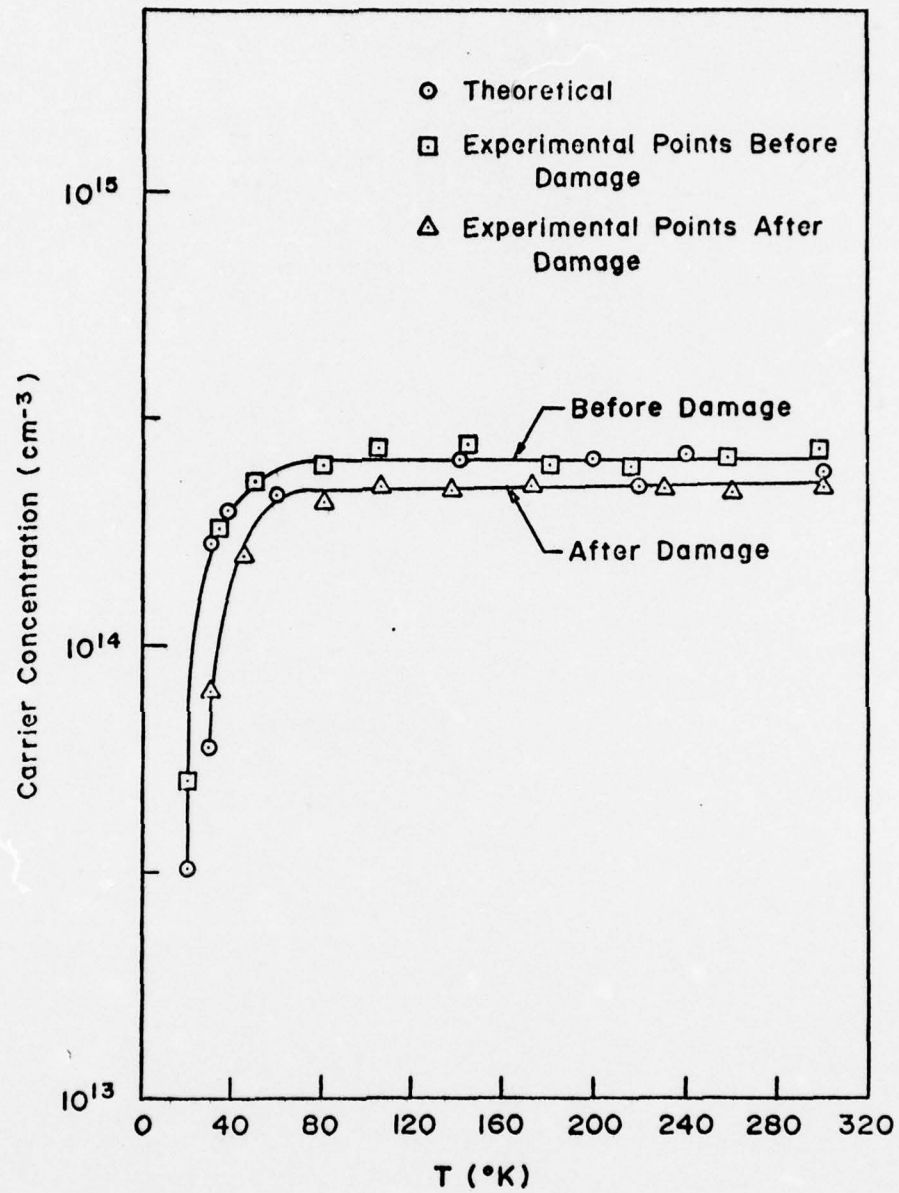
Figure 4-4. Carrier concentration versus temperature for Ge
before and after laser damage (Other parameters
are same as in Figure 4-2.)
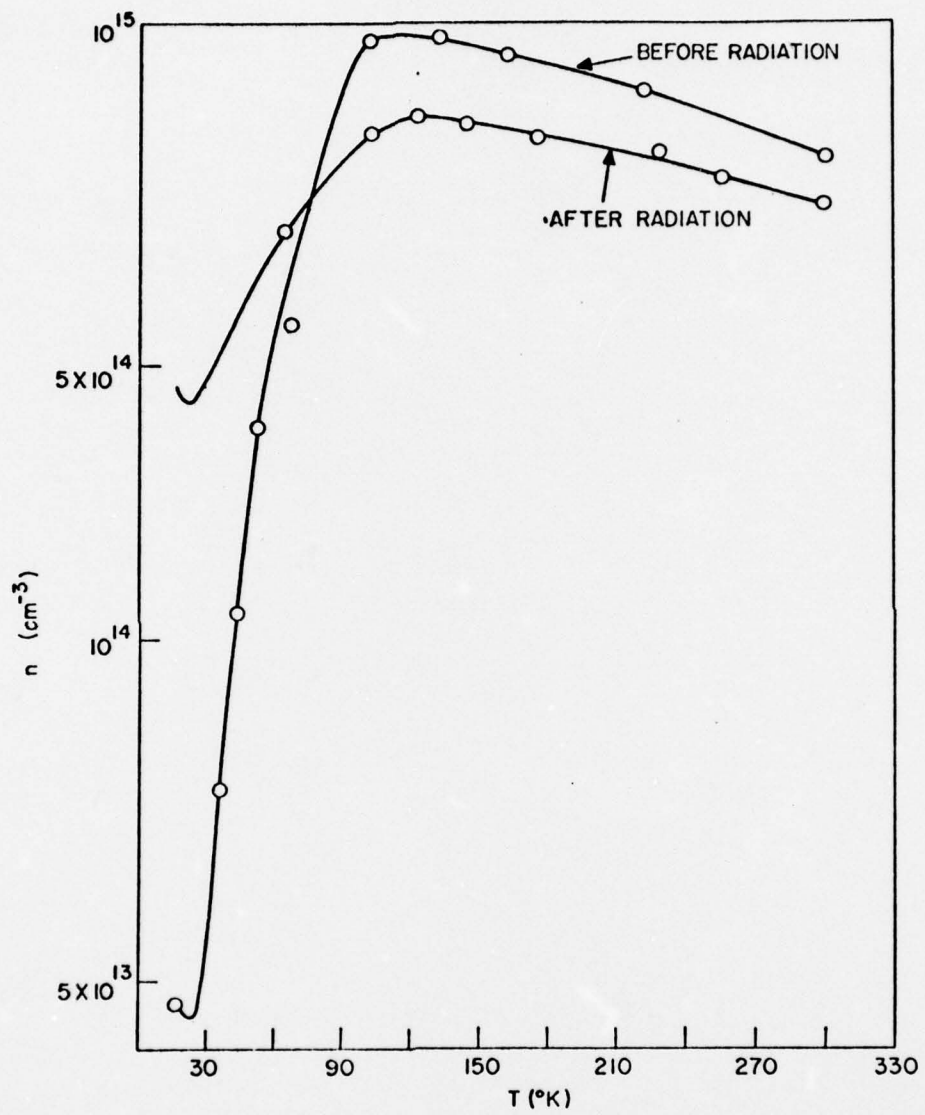
Figure 4-5. A magnified view of Figure 4-3 to show the sig-
nificant carrier removal due to laser damage

71
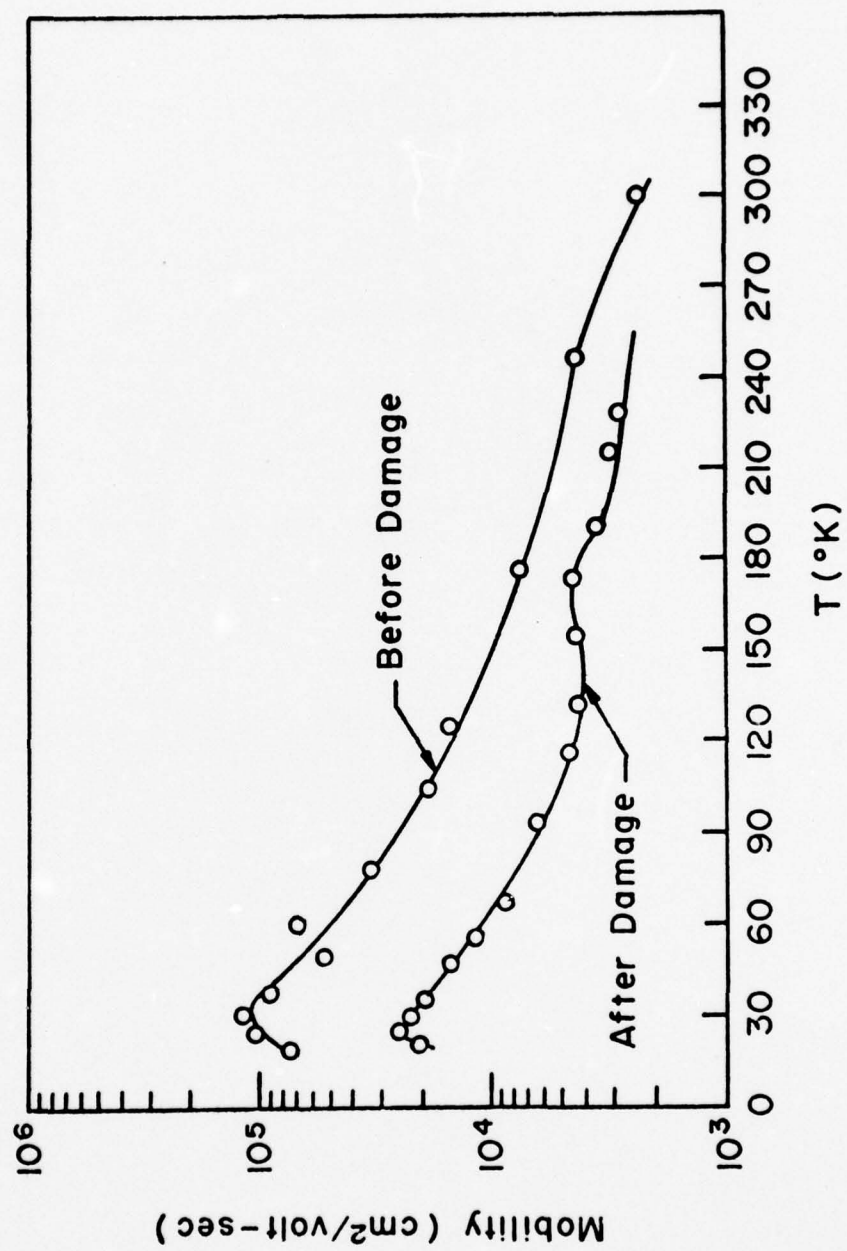
Figure 4-6. Electron mobility versus temperature for Ge before and after damage (Other parameters are same as in Figure 4-2.)

72
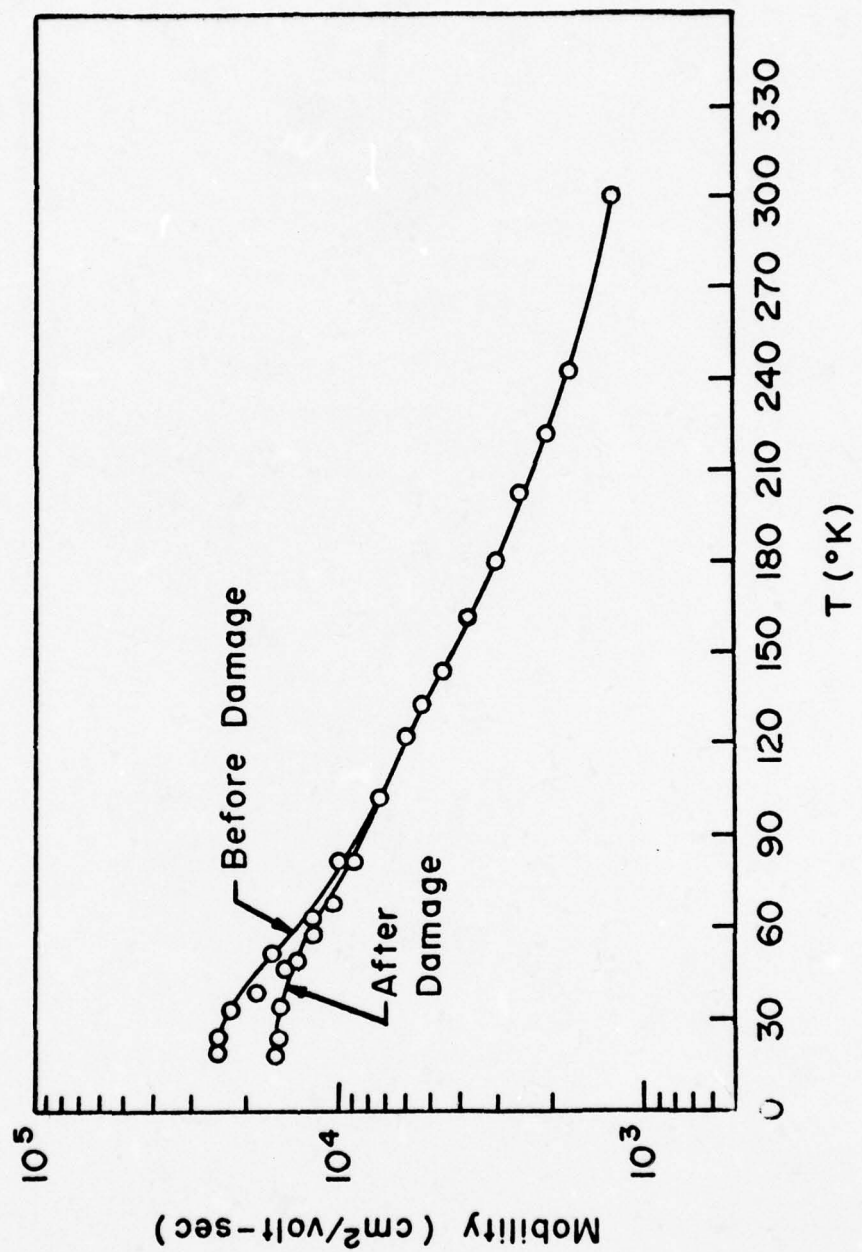
Figure 4-7. Electron mobility versus temperature for Si before and after damage (Other parameters are same as in Figure 4-3.)

73

3.   THEORETICAL EXPLANATION OF DAMAGE THRESHOLDS [2]

A systematic analysis of different damage mechanisms given in Chapter 2 shows the following.

(a) All band to band transitions are energetically forbidden, because the photon energy for CO_2 laser is only 0.117 eV, which is much smaller than any of the band gaps involved. Transitions to surface states are possible, however.

(b) Simple Joule heating is insufficient to raise the temperature of the sample to melting point in a time of about 0.1 second for which the samples were irradiated.

(c) Multiphoton absorption cross sections are too low [3] to cause any significant absorption.

(d) Damage to doped and undoped samples occurs at the same power levels. This rules out the occurrence of damage due to free carriers. Free carrier absorption, however, can be a cause of raising the electron temperature in the early stages of damage process.

(e) Lucky electron theory of avalanche cannot apply to high mobility semiconductors, because of the fact that $\omega\tau_e \gg 1$. This inequality rules out the possibility of a hard momentum-reversing collision during half period of the laser, essential for the buildup of an electron avalanche. Shatas et al. [4] have also ruled out electron avalanche as a probable damage mechanism in GaAs and NaCl crystals.

This leaves one with plasma instabilities. Upon examination

74

of several different types of plasma instabilities, it was determined that the theory of parametric instability of DuBois and Goldman [5], when combined with the theory of anomalous absorption of Dawson and Oberman [6], explains the observed damage thresholds satisfactorily.

This kind of instability can be excited in a system if the energy is fed into the solid-state plasma at a rate faster than the system can dissipate it. The intense laser beam of frequency ω_o (2.83×10^{13} Hz in this case) interacts nonlinearly with the electron plasma, that has a resonance frequency given by

$$\omega_R = \left(\omega_e^2 + 3k^2 s_e^2 \right)^{\frac{1}{2}}$$

(where ω_e is the Langmuir frequency of the electron plasma and s_e is the thermal velocity of the electron) and pumps the ion plasma at the beat frequency $(\omega_o - \omega_R)$. If ω_o and ω_R are very nearly equal, then $(\omega_o - \omega_R)$ is small and is characteristic of the ion acoustic frequency. Similarly, the laser beam can interact with the ion acoustic wave and pump the electron plasma. If this type of instability has a positive growth rate, then it can cause anomalous absorption and heating of the sample with subsequent lattice damage.

The calculation of the damage thresholds is based on finding the nonlinear susceptibility in terms of the laser beam parameters (E_o, ω_o, k_o) and electron plasma parameters (n, T, ω_e).

It was shown in Chapter 2 (see Equation 2.77)

75

$$\epsilon_L^{NL}(\vec{k},\omega) = \epsilon_L(\vec{k},\omega) - \frac{\Lambda^2}{(k^2/k_D^2)\epsilon_L(\vec{k},\omega-\omega_o)} \tag{4.1}$$

for $k \ll k_D$, $\Lambda^2 < 1$ where $\epsilon_L(\vec{k},\omega)$ is the linear longitudinal dielectric constant of the electron plasma and $\epsilon_L^{NL}(\vec{k},\omega)$ is the nonlinear dielectric constant under the action of the intense laser beam. Here

$$\Lambda^2 = \frac{1}{4}\left(\frac{\omega_p}{\omega_o}\right)^4 \frac{I_o}{nck_BT} \tag{4.2}$$

in which ω_p is the usual Langmuir frequency of the plasma and ω_o is the frequency of the incident laser field and I_o its density. n is the electron concentration of the plasma. Also, k_D is the inverse of the Debye-Huckel shielding length.

The nonlinear dielectric constant has two parts. The real part, when equated to zero, would give the resonance frequency of the plasma and is always very close to ω_o. The imaginary part gives the damping rate (γ^{NL}/ω_p)

$$\frac{\gamma^{NL}}{\omega_p} = IM \; \epsilon_L^{NL}(\vec{k},\omega_L)$$

$$= \frac{\gamma_L}{\omega_p} - \Lambda^2 Im\left(\frac{k_D^2}{k^2} \epsilon_L^{-1}(k,\omega_L - \omega_o)\right), \tag{4.3}$$

where

$$Im\left(\epsilon_L(\vec{k},\omega_L)\right) = \frac{\gamma_L}{\omega_p} \tag{4.4}$$

and is ordinary Landau damping. In the case of a solid state plasma, it can be approximated as

76

$$\frac{\gamma_L}{\omega_p} \approx \frac{1/\tau_c}{\omega_p} = \frac{1}{\omega_p \tau_c} \tag{4.5}$$

where τ_c is the collision time of the carriers with the lattice phonons.

$$\text{Im}\left[\left(\frac{k_D}{k^2}\right)^2 \varepsilon_L^{-1}(\vec{k}, \omega_L - \omega_o)\right] \text{ can be estimated by } \left(\frac{\omega_i}{\gamma_i}\right)\left(\frac{\omega_\ell}{\gamma_\ell}\right)$$

where γ_i/ω_i and γ_ℓ/ω_ℓ give the damping rates for acoustic and optical phonons, respectively [7].

Hence

$$\frac{\gamma^{NL}}{\omega_p} = \frac{\gamma_L}{\omega_p} - \Lambda^2\left(\frac{\omega_i}{\gamma_i}\right)\left(\frac{\omega_\ell}{\gamma_\ell}\right) \quad.$$

This damping rate is negative (i.e., we have the growth of instability) if

$$\Lambda^2\left(\frac{\omega_i}{\gamma_i}\right)\left(\frac{\omega_\ell}{\gamma_\ell}\right) \geq \frac{\gamma_L}{\omega_p}$$

or writing in terms of power threshold

$$P_{th} \approx 4nck_BT\left(\frac{\omega_o}{\omega_p}\right)^4\left(\frac{\gamma_L}{\omega_p}\right)\left(\frac{\gamma_i}{\omega_i}\right)\left(\frac{\gamma_\ell}{\omega_\ell}\right) \tag{4.6}$$

Now $\omega_o \approx \omega_p$ and for this to be true the plasma concentration should be of the order of 10^{18} to 10^{19} cm^{-3}. But the starting carrier concentrations here are much less than this. Therefore, a new excitation mechanism is proposed which would alleviate enough electrons from the valence band to the conduction band via a continuous distribution of surface states within the band gap. This will be disucssed at the end of this section.

In a solid state plasma Drude absorption causes the electron

77

temperature to be higher than the ion bed temperature. Therefore, one can approximate [8]

$$\left(\frac{\gamma_i}{\omega_i}\right) \simeq \frac{1}{2}\left(\frac{m_e}{m_i}\right)^{\frac{1}{2}}\left(\frac{\pi}{2}\right)^{\frac{1}{2}} \tag{4.7}$$

γ_ℓ/ω_ℓ usually lies between 10^{-1} and 10^{-2} [7], depending upon the semiconductor. This mode is more readily damped in Si and Ge than in GaAs, GaAsP, GaP and salt windows.

Using appropriate values of the damping rates, and Equation 4.6, the damage thresholds for different semiconductors have been calculated. The calculated values are compared with the experimental values in Table 4-2.

The damping ratios used in the calculations are only approximate. These ratios are difficult to estimate from theories as well as from experiments.

Table 4-2. Theoretical and Experimental Damage Thresholds for Different Semiconductors

Material	Calculated Damage Thresholds in W cm^{-2}	Experimental Damage Thresholds in W cm^{-2}
Si (n-type)	7.2×10^4	1.1×10^4
Si (p-type)	9.8×10^4	2.2×10^4
Ge	4.08×10^4	8.5×10^3
GaAs	7.14×10^3	6×10^3
GaAsP	5.7×10^3	3.5×10^3
GaP	8×10^4	1.33×10^3
KCl	$10^4 \rightarrow 10^5$	$10^4 \rightarrow 10^5$

Photon Induced Excitation

It is well known that the width of the band gap for a semiconductor is much less near the surface as compared to within the bulk, e.g., the band gap for GaAs near the surface is 0.30 eV to 0.36 eV and 1.6 eV within the bulk [9]. Also within the band gap, there is a continuous distribution of surface states having a density of about 10^{12} to 10^{14} cm^{-2} $(eV)^{-1}$. The lifetimes for these states are 3 to 4 orders longer as compared to ω_o^{-1} for CO_2 laser. The electrons in the states near the Fermi level in an n-type semiconductor are almost resonantly excited to the conduction band. The emptied states are filled again by the electrons excited by the photons from the states lying below the Fermi level. This streaming process can produce electron concentrations of 10^{18} to 10^{19} cm^{-3} within milliseconds or less. The quantum yields and transition probabilities for such processes have been calculated by Kane [10] and experimentally verified by Gobeli and Allen [11]. The quantum yield has been shown to be of the order $(h\nu-E_s)^n$ where n = 1 to 5/2, E_s is the separation between two surface states and $h\nu$ is the photon energy. This high quantum yield makes the proposed mechanism highly probable.

4. EXPLANATION OF ELECTRICAL DAMAGE [12]

Radiation damage in semiconductors produces lattice defects in the form of the interstitials, vacancies, divacancies or vacancy-impurity complexes depending upon the nature of the radiation and the semiconductor involved. In case of neutron, electron

and γ-ray damage of semiconductors, the creation of these defects can easily be explained by considering the collision between the individual radiation particle and the lattice atoms. In the CW CO_2 laser damage, however, a single photon has only .117 eV of energy and, therefore, cannot cause displacement of atoms. As discussed in the previous section, the damage mechanism in the present case is the anomalous absorption of laser energy by the solid-state electron plasma. The anomalously heated plasma gives up its energy to the lattice atoms primarily through Landau damping [13]. At the given damage thresholds the energy gained by the lattice is enough to displace 10^{19} atoms/cm^3, assuming that the displacement energy per atom is 25 eV [14]. Most of the displaced atoms end up in other normal lattice sites, while about 1 in 10^6 finally occupies an interstitial site, thereby creating interstitial-vacancy pairs. Some divacancies or vacancy-impurity complexes may also be produced in the process. The net result of the formation of these defects is the creation of localized electronic levels in the bandgap that act as trapping centers.

Earlier ideas concerning the energy levels associated with the interstitial and the vacancy were based on their single ionization energies. However, in 1951, it was shown by James and Lark-Horovitz [15] that the second ionization energies of the interstitial and vacancy also play a dominant role in determining the activation energies of the localized levels associated with the radiation damage. Based on these arguments, the following localized levels can be predicted:

(a) A shallow vacant level corresponding to the first
ionization energy of Si or Ge, located at approxi-
mately 0.05 eV below the conduction band.

(b) A deep, vacant level corresponding to the second
ionization energy of the interstitial or vacancy
in Si or Ge.

The two remaining levels lie very close to the valence band
and shall always be occupied. Predicting the precise location
of these levels with the help of theoretical calculations is ex-
tremely difficult because of the complex nature of the wave func-
tions associated with the defects and their large perturbing
effect. In the discussion that follows, we shall assume that
only the empty levels can cause any carrier removal through the
equation

electron + trap $\rightleftarrows$ occupied trap.
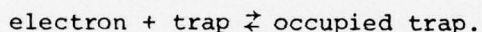
Le n be the electron concentration and N be the concentra-
tion of the deep traps. N is also the concentration of the shal-
low traps. At a given temperature, only a certain number of
shallow traps are occupied, while all the deep traps are occu-
pied at all temperatures. Let N_t be the concentration of the
occupied traps, then

$$\underbrace{n}_{\text{electron}} + \underbrace{(N - N_t)}_{\text{vacant traps}} \rightleftarrows \underbrace{N_t}_{\text{occupied traps}} . \tag{4.8}$$
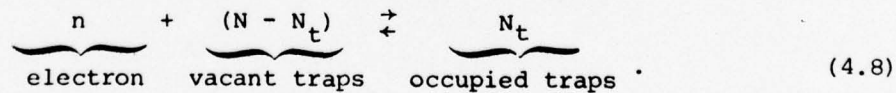
Applying the law of mass action to this reaction, one has

$$K_t = \frac{N_t}{n(n - N_t)} \tag{4.9}$$

81

or

$$N_t = \frac{nNK_t}{1 + nK_t} \qquad (4.10)$$

where K_t is a constant and can be shown to be [13]

$$K_t = \frac{h^3 \exp[E_s/k_B T]}{(16\pi m_e^* k_B T)^{3/2}} \qquad (4.11)$$

where

E_s = Depth of the shallow traps below the conduction band

T = Temperature in absolute degrees

k_B = Boltzmann constant

m_e^* = Electron effective mass.

Now at any temperature, the carrier concentration can be written as

$$n = n_o - N_t - N \qquad (4.12)$$

where n_o is the original electron concentration.

Substituting for N_t from Equation 4.10 in Equation 4.12

$$n = \frac{1}{2K_t} \left[(n_o - 2N) K_t - 1 + \sqrt{[(n_o - 2N) K_t - 1]^2 + 4K_t (n_o - N)} \right] \qquad (4.13)$$

Equation 4.13 can be used to predict carrier concentration versus temperature, provided N is known. N can be found from the mobility data as follows.

As discussed earlier, the Frankel defects act like charged scattering centers. Therefore, one can apply Brook-Herring [16] theory according to which the mobility due to ionized impurities

82

is given by

$$\mu_I = \frac{A}{2N_I B} \tag{4.14}$$

where

$$A = \frac{2^{7/2} \times (\pi)^{-3/2} (k_B T)^{3/2} \epsilon^2}{Z^2 e^3 m_e^{*\frac{1}{2}}} \tag{4.15}$$

and ϵ = Dielectric constant of the semiconductor

Z = Nuclear charge of the impurity

e = Electronic charge

$$B = \ln(1 + b) - b/(1 + b) \tag{4.16}$$

where

$$b = \frac{6(k_B T)^2 m_e^*}{\pi e^2 h^2 n_o} \tag{4.17}$$

At any temperature, lattice vibrations also contribute to scattering and the total mobility can be written as

$$\left(\frac{1}{\mu_t}\right) = \left(\frac{1}{\mu_I}\right) + \left(\frac{1}{\mu_\ell}\right) \tag{4.18}$$

where μ_ℓ is the mobility as determined by lattice vibrations.

The radiation damage does not affect the lattice scattering, therefore, any change in total mobility can be brought about only by changing the total number of charged scattering centers.

Hence

$$\Delta\left(\frac{1}{\mu_I}\right) = \Delta\left(\frac{1}{\mu_t}\right)$$

or from Equation 4.14,

83

$$\Delta \left(\frac{1}{\mu_I} \right) = \Delta \left(\frac{1}{\mu_t} \right) = \frac{2B}{A} (\Delta N_I)$$

ΔN_I gives the total number N of Frankel defects created due to the laser damage

$$N = \frac{A}{2B} \Delta \left(\frac{1}{\mu_t} \right) \tag{4.19}$$

Using Equation 4.19 and the mobility versus temperature curves at several temperatures, mean values of N for Ge and Si were determined to be 3.32×10^{13} cm^{-3} and 8.1×10^{12} cm^{-3}, respectively. Using these values of N and Equation 4.13, it is found that the predicted n versus T dependence coincides with the experimental for E_s = 0.18 eV in the case of Ge and for E_s = 0.36 eV in the case of Si (see Figures 4-3 and 4-4).

We see that the experimentally determined trap depth of 0.18 eV differs considerably from the theoretically predicted trap depth of 0.05 eV. However, theoretical prediction is based on an extremely simple hydrogenic model which is not true in actual practice. Neutron [17] and γ-ray [18] damage studies in Ge have also shown the existence of this localized level at about the same depth. Similar radiation damage studies in the case of n-type Si have shown [19, 20] the existence of two traps: one lying at 0.16 eV and the other at 0.40 eV below the conduction band, the former being produced much more frequently than the latter. Moreover, D. E. Hill [21] has found evidence for a localized state at 0.36 eV below the conduction band, which coincides with the present study.

84

REFERENCES

1. W. G. Spitzer and J. M. Whelan, "Infrared Absorption and Electron Effective Mass in n-Type Gallium Arsenide," Phys. Rev. 114, 59 (1959).

2. S. K. Gulati and W. W. Grannemann, Laser Induced Damage in Optical Materials 1976, Editors A. J. Glass and A. H. Guenther, N. B. S. Special Publication 462, Washington, D. C. (1976) p. 357.

3. R. A. Shatas, S. S. Mitra and L. M. Narducci, Laser Induced Damage in Optical Materials 1975, Editors, A. J. Glass and A. H. Guenther, N. B. S. Special Publication 435, Washington, D. C. (1975) p. 369.

4. R. A. Shatas, J. D. Stettler, L. M. Narducci, S. S. Mitra and H. C. Meyer, Laser Induced Damage in Optical Materials 1974, Editors A. J. Glass and A. H. Guenther, N. B. S. Special Publication 414, Washington, D. C. (1974) p. 200.

5. D. F. DuBois and M. V. Goldman, "Radiation Induced Instability of Electron Plasma Oscillations," Phys. Rev. Lett. 14, 544 (1965).

6. J. Dawson and C. Oberman, "High Frequency Conductivity and the Emission and Absorption Coefficients of a Fully Ionized Plasma," The Phys. of Fluids, 5, 517 (1962).

7. N. Tzoar, "Nonlinear Excitation of Density Fluctuations in Electron Plasma Systems," Phys. Rev. 164, 518 (1967).

8. B. D. Fried and L. D. Conte, The Plasma Dispersion Function, (Academic Press, inc., New York 1961).

9. R. A. Shatas, L. M. Narducci, J. L. Smith, H. C. Meyer and S. S. Mitra, Laser Induced Damage in Optical Materials 1973, Editors A. J. Glass and A. H. Guenther, N. B. S. Special Publication 387, Washington, D. C. (1973) p. 217.

10. E. O. Kane, "Theory of Photoelectric Emission from Semiconductors," Phys. Rev. 127, 131 (1962).

11. G. W. Gobeli and F. G. Allen, "Work Function, Photoelectric Threshold, and Surface States of Atomically Cleaned Silicon," Phys. Rev. 127, 150 (1962).

12. S. K. Gulati and W. W. Grannemann, "Laser (CW CO_2) Induced Electrical Damage in Ge and Si," to be published in Journal of Applied Physics, Manuscript No. 2975 R.

13. J. E. Drummond, Plasma Physics, (McGraw-Hill Book Company, New York, 1961).

14. F. Seitz and J. H. Koehler, "Displacement of Atoms During Irradiation," Solid State Physics (Editors F. Seitz and D. Turnbull), Vol. 2, 307 (1956).

15. H. M. James and K. Lark-Horovitz, "Localized Electronic States in Bombarded Semiconductors," Z. Physik. Chem. 198, 107 (1951).

16. C. Herring, "Trnasport Properties of Many Valley Semiconductors," Bell Syst. Tech. J. 34, 237 (1955).

17. J. W. Cleland, J. H. Crawford and J. C. Pigg, "Fast-Neutron Bombardment of n-Type Ge," Phys. Rev. 98, 1742 (1955).

18. J. W. Cleland, J. H. Crawford and D. K. Holmes, "Effects of Gamma Radiation on Germanium," Phys. Rev. 102, 722 (1956).

19. G. K. Wertheim, "Energy Levels in Electron Bombarded Silicon," Phys. Rev. 105, 1730 (1957).

20. E. Sander and L. C. Templeton, "Energy Levels Introduced into Silicon by Electron Irradiation," Bull. Am. Phys. Soc. 3, 375 (1958).

21. D. E. Hill and K. Lark-Horovitz, "Gamma Irradiation of n-Type Silicon," Bull. Am. Phys. Soc. 3, 142 (1958).

CHAPTER 5

RESULTS: Nd:YAG LASER DAMAGE

This chapter presents the results on laser damage of semi-
conductors at 1.06 μm wavelength. The beam divergence was
2×10^{-4} radians and its duration between half power points was
~35 ns. The pulse shape was Gaussian in space and time, as shown
in Figure 5-1.

|← 100 n-sec |←
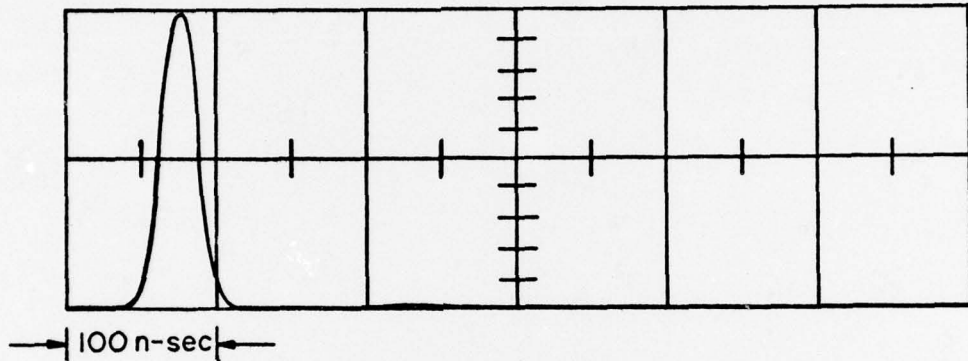
Figure 5-1. Nd:YAG Laser Pulse (width ~35 ns)

The manner in which the samples were irradiated is shown in
Figure 5-2. Different neutral filters were used in the path of
the beam to adjust the irradiance at the sample. A reflected beam
off a beam splitter was fed to an energy meter to measure the
energy incident on the sample. The criteria used for damage are
the same as in References [1, 2].

A lens of focal length 50 cm was used to focus the beam on
the sample. The size of the focal spot on the sample is calcu-
lated from [3]

$$s = f \cdot \theta \tag{5.1}$$

87
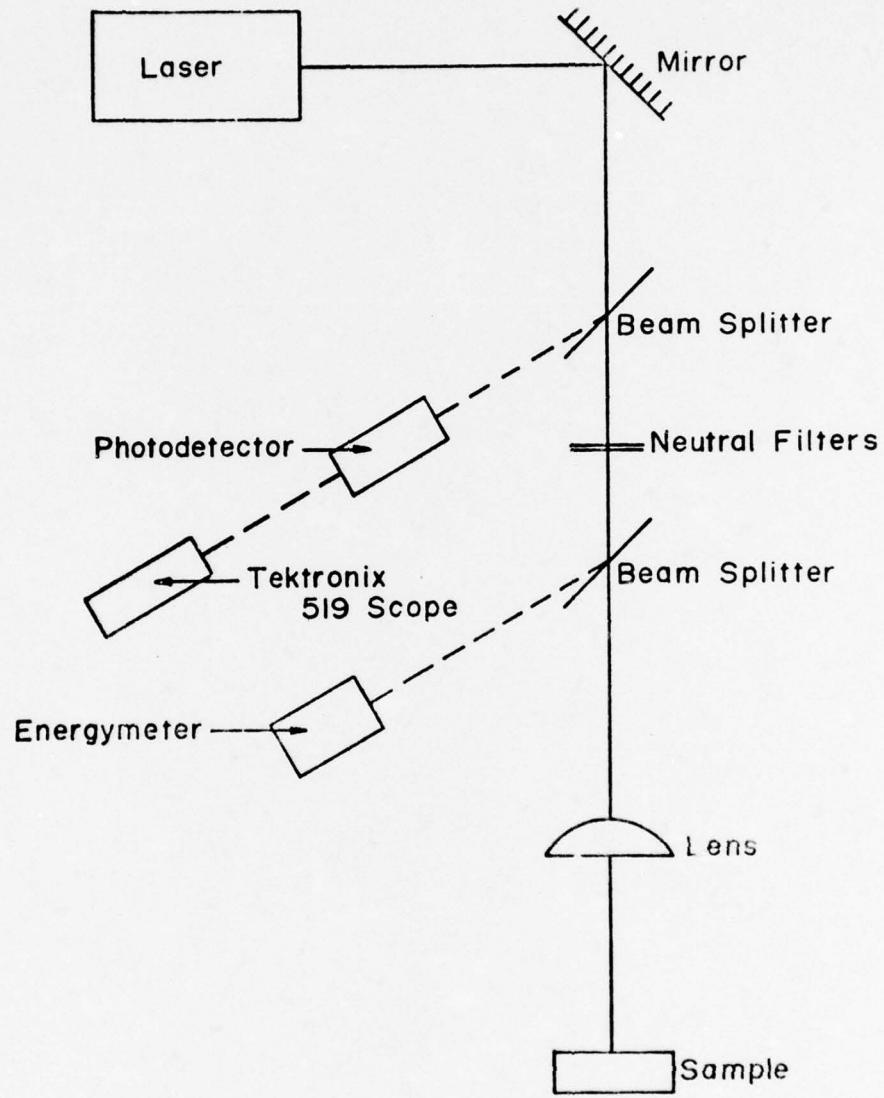
Figure 5-2.   Experimental arrangement used
to radiate the samples

where f is the focal length of the lens and θ, the beam divergence.
Equation 5.1 is true only at very small distances from the laser.
This condition was satisfied in the experimental arrangement. Dif-
ferent semiconductors with their solid state parameters and their
respective experimental damage thresholds are shown in Table 5-1.

Table 5-1. Damage threshold for different
semiconductors at 1.06 microns

| Semiconductor	Mobility $(cm^2(V/sec)^{-1})$	Carrier concentration (cm^{-3})	Band gap (eV)	Experimental damage thresholds $(W\ cm^{-2})$
Si	1200	1.3×10^{15}	1.10	7.31×10^8
Ge	2300	4×10^{14}	0.79	1.59×10^8
GaAs	3500	1×10^{16}	1.40	2.24×10^8
$GaAs_xP_{1-x}$ (x = .3)	2000	2×10^{17}	1.70	6.25×10^8
GaP	110	$\sim 10^{18}$	2.20	2.80×10^9

1.   EXPLANATION OF DAMAGE THRESHOLDS

It was shown in Chapter 4 that the damage mechanism for
CW CO_2 laser was parametric instability of the type formulated by
DuBois and Goldman. The necessary plasma was produced by photon
induced excitation and was time dependent. Due to the short dura-
tion of the laser pulse ($\sim 3.5 \times 10^{-8}$ sec) in the present case
photon induced excitation would be negligible.

For parametric instability to grow, an electron concentration
of 1.29×10^{20} cm^{-3} is required in the plasma in the case of Si and

89

3.96 x 10^{19} in the case of Ge. However, in the case of Nd:YAG
laser the energy of a single photon is 1.17 eV, which is higher
than the band gap of either Si (1.10 eV) or Ge (0.79 eV). It is,
therefore, clear that band to band transitions (indirect in the
case of Ge and Si) would be very dominant. The incident photon
flux in the case of Si is 1.56 x 10^{29} photons per second per cm^3,
and 3.4 x 10^{28} photons per second per cm^3 in the case of Ge. [The
photon flux in $cm^{-2}sec^{-1}$ has been divided by the thickness of the
sample.] Hence, during the duration of the pulse, there will be
5.41 x 10^{21} transitions/cm^3 in Si and 1.19 x 10^{21} cm^{-3} in Ge. The
number of these transitions is enough to provide the required
plasma concentration.

Such band to band transitions are energetically forbidden in
GaAs, $GaAs_1P_{1-x}$ (x = 0.3) and GaP, whose band gaps are higher than
the photon energy of 1.17 eV. But because of the high electric
fields associated with the incident laser flux, it is found that
Zener type tunneling across the band gap barrier can give appre-
ciable tunneling rates to account for the electron plasma in GaAs,
$GaAs_xP_{1-x}$ and GaP.

Zener Tunneling Rate

In this section an expression for Zener tunneling [4] rate
using Heisenberg uncertainty principal and WKB approximation will
be derived. Using this expression, we shall find the tunneling
rates for GaAs, $GaAs_xP_{1-x}$ and GaP.

It is known that a Bloch electron can have energies only in

certain allowed bands. However, in the presence of an electric

field an electron can jump from one band to another, provided it

can travel freely through a certain distance d, given by

$$d = \frac{E_g}{|e\vec{E}|} \tag{5.2}$$

where E_g is the forbidden band gap and $\vec{E}$ is the applied electric

field.

Quantum mechanically, this implies that the wave function

across the band gap is exponentially decreasing instead of being

zero at the zone boundaries. This is shown in Figure 5-3.
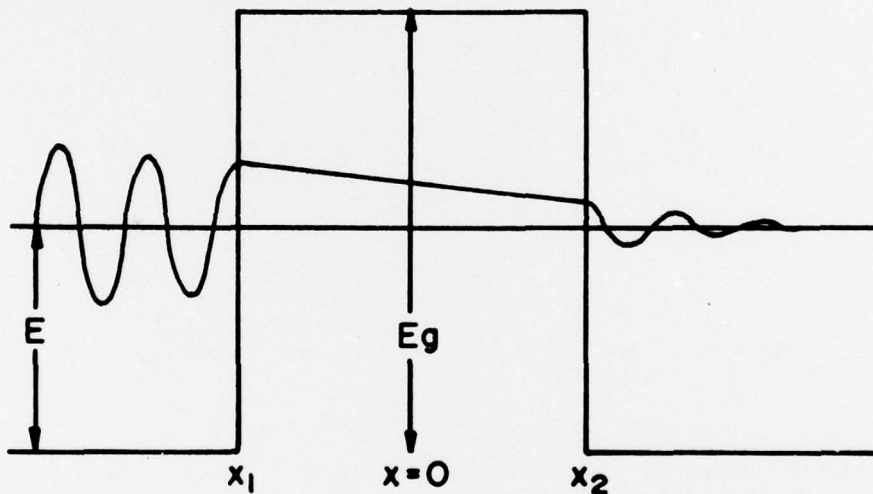
Figure 5-3. Tunneling through a potential barrier

Applying WKB approximation, the tunneling probability [5]

can be written as

$$T = \exp\left[-2 \int_{x_1}^{x_2} \beta(x)\,dx\right] \tag{5.3}$$

91

where $\beta = \sqrt{\dfrac{2m}{\hbar^2} \; (V(x) - E)}$ (5.4)

and $V(x)$ depends on the shape of the barrier and is determined both by the nature of the semiconductor and the applied electric field.

To calculate the tunneling rate, one must consider the nature of the wave function in the forbidden energy range.

Consider Schroedinger equation,

$$-\frac{h^2}{2m} \nabla^2 \psi + \{V(\vec{r}) - E\}\psi = 0$$ (5.5)

Try a solution of the form

$$\psi = \sum_{\vec{g}} \alpha_{\vec{k}-\vec{g}} \; e^{i(\vec{k}-\vec{g}) \cdot \vec{r}}$$ (5.6)

where g is a reciprocal lattice vector. Substituting Equation 5.6 in Equation 5.5, produces

$$\left(E^O_{\vec{k}-\vec{g}} - E(\vec{k})\right) \alpha_{\vec{k}-\vec{g}} + \sum_{\vec{g}'} V_{\vec{g}'-\vec{g}} \, \alpha_{\vec{k}-\vec{g}'} = 0$$ (5.7)

where $V(x)$ has been expanded in its fourier series

$$V(\vec{r}) = \sum_{\vec{g}'} V_{\vec{g}'-\vec{g}} \, e^{i(\vec{g}'-\vec{g}) \cdot \vec{r}}$$ (5.8)

and $\quad E^O_{\vec{k}-\vec{g}} = \dfrac{\hbar^2}{2m} \, (\vec{k} - \vec{g})^2$ (5.9)

These equations are true for all values of g including $g = 0$ and $g' = 0$. When the perturbation due to the electric field is small, then all α_{k-g} are small except α_k. This assumption breaks down near a zone boundary because of the fact that a Bragg reflection occurs. Hence to construct a stationary wave we must

consider both the incident wave and the diffracted wave on equal footing.

Ignoring all coefficients except these two in Equation 5.7,

$$\left\{ E^O_{\vec{k}} - E(\vec{k}) \right\} \alpha_{\vec{k}} + V_{\vec{G}} \alpha_{\vec{k}-\vec{G}} = 0 \tag{5.10}$$

$$V_{-\vec{G}} \alpha_{\vec{k}} + \left\{ E^O_{\vec{k}-\vec{G}} - E(\vec{k}) \right\} \alpha_{\vec{k}-\vec{G}} = 0 \tag{5.11}$$

where

$$\left| \vec{G} \right| = \frac{2\pi}{a} \tag{5.12}$$

and $E^O = \dfrac{\hbar^2}{2m} \left(\dfrac{G}{2} \right)^2$ (5.13)

Equations 5.10 and 5.11 will have a non-trivial solution if

$$\left[E^O_{\vec{k}-\vec{G}} - E(k) \right] \left[E^O_{\vec{k}} - E_{\vec{k}} \right] - \left| V_G \right|^2 = 0$$

or $\left. \dfrac{\hbar^2}{2m} (\vec{k} - \vec{G})^2 - E \right] \left[\dfrac{\hbar^2}{2m} \vec{k}^2 - E \right] = \left| V_G \right|^2$ (5.14)

For real k, this equation has no solution for

$$E^O - \left| V_G \right| < E < E^O + \left| V_G \right| \tag{5.15}$$

However, this is the region of interest here. Let

$$\vec{k} = \frac{G}{2} + \kappa \quad \text{and } E = E^O + \xi$$

where κ and ξ are small

Making this substitution in Equation 5.14, one gets

$$\kappa^2 = \frac{2m}{\hbar^2} \left[\frac{\xi^2 - \left| V_G \right|^2}{4E^O} \right] \tag{5.16}$$

From Equation 5.16, we see that κ can be imaginary if

$$\xi^2 < \left| V_G \right|^2.$$

93

Then β of Equation 5.4 is given by

$$\beta = \sqrt{\frac{2m}{\hbar^2} \frac{\left(|V_G|^2 - \xi^2\right)}{4E_o}} \qquad (5.17)$$

Now using Equation 5.17 and Equation 5.3, the tunneling probability is given by

$$T = \exp\left[- \int_{x_1}^{x_2} 2 \cdot \sqrt{\frac{2m}{\hbar^2}\left(\frac{|V_G|^2 - \xi^2}{4E^o}\right)} \ dx \ . \right] \qquad (5.18)$$

Now $\xi = eEx$ \qquad (5.19)

where E now is applied electric field. From Equation 5.2,

$$|E_g|^2 = 4|V_G|^2 = e^2 E^2 d^2$$

or $\quad |V_G|^2 = \dfrac{e^2 E^2 d^2}{4}$ \qquad (5.20)

Hence Equation 5.18 with the help of Equations 5.19 and 5.20 becomes

$$T = \exp\left\{- 2 \int_{-d/2}^{+d/2} \sqrt{\frac{2m}{4\hbar^2 E^o} |V_G|^2 \left(1 - \frac{4x^2}{d^2}\right)}\right\} \qquad (5.21)$$

Performing the integration and making use of Equations 5.12 and 5.13, one gets

$$T = \exp\left[- \frac{ma E_g^2}{4\hbar^2 eE}\right] \qquad (5.22)$$

where a is the lattice constant.

In actual practice m must be replaced by the electron effective mass m_e^*

94

$$\therefore \quad T = \exp\left(-\frac{m^*_e a E_g^2}{4\hbar^2 eE}\right) \tag{5.23}$$

To obtain the total tunneling probability one must multiply T by the number of Bragg reflections that can occur within a lattice period in one second. This is done by applying Heisenberg's uncertainty principle. If the electron is allowed to move freely within the solid through a spacing a before its momentum is totally randomized, electric field has accelerated it to an energy of eEa so that the electron can have an energy uncertainty of eEa. But by the uncertainty principle

$$\Delta E \Delta t \sim h$$

$$\therefore \quad \Delta t \sim \frac{h}{eEa}$$

and hence the frequency with which the Bragg reflection can occur is

$$\nu_b = \frac{1}{\Delta t} = \frac{eEa}{h} \tag{5.24}$$

From Equations 5.23 and 5.24, the tunneling rate is given by

$$w(\sec^{-1}) = \frac{eEa}{h} \exp\left\{-\frac{m^*_e a E_g^2}{4\hbar^2 eE}\right\} \tag{5.25}$$

which is Zener's original formula.

Now tunneling rates for GaAs, $GaAs_x P_{1-x}$ and GaP using Equation 5.25 and the electric fields calculated from the experimental damage thresholds will be calculated. The following expression is used to find the electric field from the damage threshold.

$$E_{th} = \sqrt{\frac{8\pi P_{th}}{c}}\left(\frac{2}{1+\sqrt{\epsilon}}\right) \tag{5.26}$$

95

The values for the effective masses were taken from Reference [6], the lattice constants from Reference [7] and the band gaps from Reference [8].

The calculated tunneling rates are listed in Table 5-2. Using these tunneling rates one can find the tunneling probability over the duration of the pulse which is 3.5×10^{-8} seconds. Assuming the concentration of the electrons in the valence band to be of the order of 10^{22} cm^{-3}, one can estimate the total number of electrons per cm^3 that can tunnel to the conduction band through this process. This number along with the plasma concentration required for the parametric instability is shown in Table 5-3. It is seen from this table that the electrons tunneling to the conduction band are enough to cause the onset of the parametric instability.

Calculation of the Damage Thresholds

It was shown in Chapter 4 that the onset of parametric instability occurs at a power threshold of

$$P_{th} = 4\pi n c k_B T \left(\frac{\gamma_L}{\omega_p} \right) \left(\frac{\gamma_\ell}{\omega_\ell} \right) \qquad \text{[See Equation 4.6.]} \qquad (5.27)$$

In this equation damping rate

$$\left(\frac{\gamma_i}{\omega_i} \right)$$

has been omitted, because over the duration of the pulse the energy damped due to this mode is negligible.

As before, Landau damping [9] can be approximated as

Table 5-2. Tunneling rates for different semiconductors at 1.06 microns

Semiconductor	Effective mass m_e^*/m	Lattice constant a (10^{-8} cm)	Dielectric constant	Band gap (eV)	E_{TH} (V cm^{-1})	Tunneling rate (sec^{-1})
GaAs	0.080	5.65	13.10	1.40	1.78×10^5	2.07×10^5
GaAs$_x$P$_{1-x}$	0.110	5.50	9.00	1.70	3.43×10^5	2.66×10^5
GaP	0.130	5.45	8.45	2.20	7.44×10^5	2.79×10^6

Table 5-3. Plasma concentration required for onset of parametric instability

Semiconductor	Tunneling probability	Electrons tunneling to the conduction band (cm^{-3})	Plasma concentration required (cm^{-3})
GaAs	7.25×10^{-3}	7.25×10^{19}	8.32×10^{19}
GaAs$_x$P$_{1-x}$	9.31×10^{-3}	9.31×10^{19}	1.09×10^{20}
GaP	9.77×10^{-2}	9.77×10^{20}	1.28×10^{20}

$$\left(\frac{\gamma_L}{\omega_p}\right) \approx \frac{1}{\omega_p \tau_e} \tag{5.28}$$

and $\dfrac{\gamma_\ell}{\omega_\ell}$

(damping due to optical phonons) usually lies between 10^{-1} and 10^{-2} [10]. Damping due to this mode is more dominant in III-V compounds as compared to those in Si and Ge. In fact, in Si and Ge it can be taken as 1 under the present conditions.

In Table 5-4, the results of the calculations of damage thresholds in comparison to the experimental results are shown. It is seen from this table that there is a reasonable agreement between the theoretical and experimental damage thresholds. The fact that the calculated thresholds are slightly higher than the experimental is due to the neglect of the damping mechanism

$$\left(\frac{\gamma_i}{\omega_i}\right)$$

due to the acoustic branch of the lattice spectrum.

Shatas et al.[11] has done similar calculations of tunneling rate and has tried to explain the pulsed CO_2 laser damage in GaAs, by using results of the modified two stream instability formulated by Kaw and Dawson [12], according to which the damage will occur when

$$v_E \gtrsim 6 \ s_e \left(1 + \frac{T_i}{T_e}\right)^{\frac{1}{2}} \left(\frac{\nu_c}{\omega_R}\right)^{\frac{1}{2}} \tag{5.29}$$

where

$$v_E = \frac{eE}{m\omega_o}$$

Table 5-4. Theoretical and experimental damage threshold for various semiconductors at 1.06 microns

Semiconductor	Plasma density n (cm^{-3})	$\dfrac{\gamma_L}{\omega_p}\left(\dfrac{\gamma_\ell}{\omega_\ell}\right) = \left(\dfrac{1}{\omega_p \tau_c}\right)\left(\dfrac{\gamma_\ell}{\omega_\ell}\right)$	Calculated damage threshold (W cm^{-2})	Experimental damage threshold (W cm^{-2})
Si	1.29×10^{20}	6.00×10^{-3}	1.17×10^{9}	7.31×10^{8}
Ge	3.96×10^{19}	1.62×10^{-3}	0.97×10^{8}	1.59×10^{8}
GaAs	8.32×10^{19}	2.35×10^{-3}	2.95×10^{8}	2.24×10^{8}
GaAs$_x$P$_{1-x}$	1.09×10^{20}	4.08×10^{-3}	6.71×10^{8}	6.25×10^{8}
GaP	1.28×10^{20}	2.53×10^{-2}	4.88×10^{9}	2.80×10^{9}

s_e = electron thermal velocity

ν_e = collision frequency of the electron

$$\omega_R^2 = \omega_p^2 + k^2 s_e^2 ,$$

where k is the wave vector of the interacting laser beam.

Equation 5.29 can easily be translated in terms of threshold power

$$P_{th} = \frac{cE^2}{8\pi} \left(\frac{1 + \sqrt{\epsilon}}{2} \right)^2$$

$$= \frac{c}{8\pi} \left(\frac{1 + \sqrt{\epsilon}}{2} \right)^2 \frac{m^2 \omega_o^2}{e^2} \cdot 6 \cdot s_e^2 \left(1 + \frac{T_i}{T_e} \right) \left(\frac{\nu_c}{\omega_R} \right) \qquad (5.30)$$

As pointed out by Kaw and Dawson, this equation holds only if $T_e \gg T_i$ and this is not true in the present problem or in the problem to which Shatas applied this result. Shatas et al. incorrectly assumed that $T_e \sim T_i$ and calculate the damage thresholds for GaAs for pulsed CO_2 laser damage. A simple calculation of damage threshold for GaAs gives 9.4×10^9 W cm^2 and is two orders higher than the experimental value.

Another type of photon-plasmon instability has been formulated by Gersten and Tzoar [13]. They arrive at a threshold condition

$$P_{th} = \frac{cE^2}{32\pi} (1 + \sqrt{\epsilon})^2$$

$$= \frac{c}{32\pi} (1 + \sqrt{\epsilon})^2 \frac{4}{3} \frac{E_g \omega_o}{\mu \cdot e} \qquad (5.31)$$

Using this formula for GaAs, one arrives at a damage threshold of $\sim 4 \times 10^{14}$ W cm^2, which is much higher than the experimental

value. Hence we can conclude that the damage process is most likely a parametric instability of the type formulated by DuBois and Goldman.

REFERENCES

1. R. A. House, "The Effects of Surface Structural Properties on Laser Induced Damage at 1.06 Micrometers," Ph.D. Thesis, Air Force Institute of Technology, Air University, U. S. Air Force, WPAFB, Ohio (1975).

2. J. R. Bettis, "Laser Induced Damage as a Function of Dielectric Properties at 1.06 µm," Ph.D. Thesis, Air Force Institute of Technology, Air University, U. S. Air Force, WPAFB, Ohio (1975).

3. J. F. Ready, Effects of High Power Laser Radiation, (Academic Press, New York 1971) p. 19.

4. C. Zener, "A Theory of Electric Breakdown of Solid Dielectrics," Proc. Roy. Soc. (London), 145, 523 A (1934).

5. J. M. Ziman, Principles of the Theory of Solids, (Cambridge University Press 1965) p. 163.

6. M. Cardona, "Band Parameters of Semiconductors with Zinc Blende, Wurtzite, and Germanium Structure," J. Phys. Chem. Solids, 24, 1543 (1963).

7. CRC Handbook of Chemistry and Physics, 56th Edition, (CRC Press, 1975-1976) p. E-101.

8. R. K. Willardson and A. C. Beer (Editors), Semiconductors and Semimetals (Optical Properties of III-V Compounts, Vol. 3, (Academic Press, New York and London 1967).

9. F. F. Chen, Introduction to Plasma Physics, (Plenum Press, New York, London, 1974) p. 211.

10. N. Tzoar, "Nonlinear Excitation of Density Fluctuations in Electron Phonon Systems," Phys. Rev. 164, 518 (1967).

11. R. A. Shatas, L. M. Narducci, J. L. Smith, H. C. Meyer and S. S. Mitra, Laser Induced Damage in Optical Materials 1973, Editors A. J. Glass and A. H. Guenther, N.B.S. Special Publication 387, Washington, D. C. (1973) p. 217.

12. P. K. Kaw and J. M. Dawson, "Laser Induced Anomalous Heating of a Plasma," The Phys. of Fluids, 12, 2586 (1969).

13. J. I. Gersten and N. Tzoar, "Parametric Excitation of Plasma Instabilities in Semiconductors," Phys. Rev. Lett., 27, 1650 (1971).

CHAPTER 6

CONCLUSION

Laser induced damage in semiconductors is, in principle, similar to particle and γ-ray damage. In all cases, there is lattice damage which causes degradation in the electrical properties such as carrier mobility, carrier concentration and carrier lifetime. In spite of this apparent similarity, there are some very important differences that must be noted. While the amount of damage is directly proportional to the incident particle flux or the γ-ray intensity, a sharply defined power level exists at which laser damage can occur. Also, particle and γ-ray damage anneals faster than laser induced damage. This proves that the fundamental damage mechanism in laser damage is different than in the particle and the γ-ray damage.

The experimental damage thresholds are found to be different at different laser wavelengths. The various semiconductors, e.g. Si, Ge, GaAs, $GaAs_xP_{1-x}$ and GaP, when radiated with CW CO_2 laser radiation were all damaged at power thresholds of a few kW/cm^2, the irradiation time being 0.10 second. When a systematic analysis of different damage mechanisms is made, it is found that the band to band transitions, the multiphoton absorption, the free carrier absorption or the lucky electron theory of avalanche cannot explain the experimentally observed damage thresholds. This leaves one with the plasma instabilities. It is found that semiconductors can be treated as containers of electron plasma that behave similarly to gaseous plasmas. The observed damage thresholds can be

103

satisfactorily explained by applying the theory of parametric instability of the type formulated by DuBois and Goodman. This instability causes anomalous increases in the semiconductor resistivity causing anomalous absorption as suggested by Kaw and Dawson.

The pre-condition for the onset of the parametric instability at 10.6 μm is a plasma concentration of 10^{17} to 10^{18} electrons cm^{-3}. Also Λ^2 (a parameter defined in Chapter 2) should be less than 1.0. The latter condition is found to be easily satisfied, while the required plasma concentration is achieved by photon induced excitation of valence electrons to the conduction band through a continuous distribution of Shockley surface states. The time required for the plasma concentration to build up to 10^{17} to 10^{18} cm^{-3} is of the order of a few milliseconds. There is enough time available for this to happen in the case of CW CO_2 radiation damage. This mechanism cannot account for a solid state plasma concentration of 10^{19} to 10^{20} electrons cm^{-3} required for the onset of parametric instability at 1.06 μm because of the very short duration of the pulse. The experimentally determined surface damage thresholds at 1.06 μm for nanosecond pulses were of the order of 10^8 to 10^9 W/cm ^{2}. These damage thresholds were higher for higher band gap semiconductors. As the energy of a single photon at 1.06 μm is 1.17 eV and the incident photon flux is of the order of 10^{20} to 10^{21} cm^{-3}, the required plasma concentration can be achieved through direct or indirect band to band transitions in the cases of Ge and Si. Such transitions are energetically forbiden in GaAs, $GaAs_xP_{1-x}$ and GaP because of the higher band gaps

104

of these semiconductors. A simple calculation shows that the longitudinal electric field associated with a flux of 10^9 W cm^{-2} is of the order of 10^5 V/cm. The Zener tunneling rates at this value of the electric field are found to be of the order of 10^5 to 10^6 sec^{-1}, giving a tunneling probability of 10^{-2} to 10^{-3} over the duration of the pulse. Because there are about 10^{22} electrons cm^{-3} in the valence band of any one of these semiconductors, the number of electrons that tunnel to the conduction band is 10^{19} to 10^{20} cm^{-3}, thus giving the required plasma concentration for the onset of the parametric instability at 1.06 μm.

In practice, damage is found to occur both at the surface and within the bulk of the semiconductor. This creates defects in the form of interstitial and vacancy pairs, giving rise to the localized traps within the band gap. These traps are found to be more active at lower temperatures than at room temperature, as seen from the experimental Hall mobility versus temperature curves. Due to this reason, these defects can be considered as scattering centers similar to ionized impurities. Both in Germanium and Silicon, it is found that the mobility decrease due to CW CO_2 laser damage is about 30 to 50 percent, and also there is significant carrier removal in these semiconductors. In this respect, therefore, the laser damage is similar to the particle and the γ-ray damage. These results on mobility and carrier concentration can be explained by applying the model of James and Lark-Horovitz, assuming the creation of localized levels at 0.18 eV below the conduction band in the case of Ge and 0.36 eV in the case of Si.

105